Technische Universität München

Lehrstuhl für Tierphysiologie und Immunologie

Shaping effector and memory T cell differentiation through the immunosuppressive drug leflunomide

Stefanie Sarah Scherer

Vollständiger Abdruck der von der Fakultät Wissenschaftszentrum Weihenstephan für Ernährung, Landnutzung und Umwelt der Technischen Universität München zur Erlangung des akademischen Grades eines Doktors der Naturwissenschaften genehmigten Dissertation.

Vorsitzende/-r: Prof. Dr. Benjamin Schusser

Prüfende/-r der Dissertation:

1. Prof. Dr. Dietmar Zehn

2. Prof. Dr. Percy A. Knolle

3. Prof. Dr. Vigo Heissmeyer

Die Dissertation wurde am 12.11.2018 bei der Technischen Universität München eingereicht und durch die Fakultät Wissenschaftszentrum Weihenstephan für Ernährung, Landnutzung und Umwelt am 01.07.2019 angenommen.

Für Martha, Josef, Lotte und Samuel

Table of Contents

1. Zusammenfassung

Nach Stimulation mit Antigenen differenzieren sich naive CD8 $^{+}$ T-Zellen in terminale Effektor- oder langlebige Gedächtnis-T-Zellen. Obwohl viel über diese Differenzierung bekannt ist, sind die genauen Mechanismen, die diese Diversität kontrollieren, noch nicht vollständig verstanden.

In dieser Arbeit demonstrieren wir, dass die spezifische Hemmung des Pyrimidin-Biosyntheseenzyms Dihydroorotatdehydrogenase (DHODH) durch pharmakologische Behandlung mit Leflunomid ein Hauptregulator der Effektor- und Gedächtnis CD8 $^{+}$ T-Zelldifferenzierung ist. Die Inhibition der Pyrimidinsynthese blockiert selektiv die Effektor-T-Zell-Differenzierung, während Gedächtnisvorläufer und langlebige Gedächtnis-T-Zellen unverändert in ihrer Anzahl, Funktion und transkriptionellem Profil erhalten bleiben. Ein Zugang zu den frühesten Gedächtnisvorläuferzellen ermöglicht es uns, den frühen Verzweigungspunkt von Effektor- und Gedächtnis-T-Zellen zu untersuchen, und wir zeigen, dass sich diese beiden Zellarten innerhalb der ersten Teilungsrunden nach T-Zell-Aktivierung separieren.

Durch zeitliche Steuerung der Leflunomid-Behandlung konnten wir weiterhin die bedeutsame Beobachtung machen, dass Effektor-T-Zellen nur in einem frühen engen Zeitfenster während der T-Zell-Aktivierungsphase gegenüber einer Pyrimidinrestriktion empfindlich sind. Darüber hinaus scheint die Pyrimidinrestriktion zu einer Störung des T-Zell-Metabolismus zu führen, die Effektor-, nicht aber Gedächtnis-T-Zellen betrifft.

Desweiteren liefern unsere Ergebnisse starke Implikationen mit klinischer Relevanz, da sie den Wirkungsmechanismus von Leflunomid klären. Unsere Beobachtung, dass voraktivierte T-Zellen in Leflunomid-gesättigten Mäusen in der Lage sind sich stark zu vermehren, wirkt der bisherigen Annahme entgegen, dass Leflunomid Autoimmunerkrankungen abschwächt, indem es einen Proliferationsstopp aktivierter T-Zellen verursacht. Im Gegensatz dazu weisen unsere Ergebnisse stark darauf hin, dass Leflunomid die Expansion und Differenzierung von zytotoxischen Effektor-T-Zellen selektiv blockiert. Eine Blockade der Effektor-, aber nicht Gedächtnis-T-Zellen Differenzierung könnte einen starken Rückfall bewirken, wenn es zu einer Unterbrechung der Leflunomidtherapie käme.

Zusammenfassend wurden in dieser Studie i) ein neuer Wirkungsmechanismus von Leflunomid, ii) die frühe Verzweigung von Effektor- und Gedächtnis-T-Zellen und iii) ein neuer metabolischer Kontrollpunkt identifiziert, welcher für das selektive Targeting der T-Zell-Differenzierung verwendet und dadurch die Verbesserung von T-Zell-vermittelten klinischen Therapien und Impfungen bewirken kann.

2. Abstract

After stimulation with antigen, naïve $CD8^+$ T cells branch into terminal effector or long-lived memory T cells. Although much has been learned about the differentiation of effector and memory $CD8^+$ T cells the precise mechanisms that control this diversity are still only partially understood.

In this study we demonstrate that specific inhibition of the pyrimidine biosynthetic enzyme dihydroorotate dehydrogenase (DHODH) through pharmacological treatment with leflunomide is a major regulator of effector and memory $CD8^+$ T cell differentiation. Restricting pyrimidine levels selectively blocks effector T cell differentiation while memory precursor and long-lived memory T cells remain number, functional and transcriptional wise unaltered. Having access to the earliest memory precursor allows us to investigate the early branching point of effector and memory T cells and we demonstrate that effector and memory precursor T cells indeed separate within the first rounds of division after T cell activation.

By timing the leflunomide treatment we further made the important observation that effector T cells are sensitive to pyrimidine starvation only in an early narrow window during the T cell activation phase. Furthermore, restrictions in pyrimidine levels seem to trigger perturbations in the T cell metabolism, which affect effector but not memory T cells.

Additionally, we observed that pre-activated T cells are able to robustly proliferate in leflunomide-saturated mice. This result has strong implications for clinical medicine as it counteracts the assumption that leflunomide simply dampens autoimmune disorders by causing a proliferation arrest of activated T cells. In contrast, we provide compelling evidence that leflunomide selectively blocks the expansion and differentiation of cytotoxic effector T cells. Blocking effector but not memory T cells could lead to strong rebounds after leflunomide treatment interruption.

Aggregating our results together, this study identifies i) a new mechanism of action of leflunomide, ii) the early branching of effector and memory T cells and iii) a novel metabolic checkpoint for the selectively targeting of T cell differentiation, that can be used to improve current and new T cell mediated clinical therapies and vaccinations.

3. Introduction

3.1 Vaccinations and the implication for a better understanding of the effector and memory T cell differentiation

The immune system constitutes a complex arrangement of cells and molecules that protect the organism against infectious diseases. Key players of the adaptive cellular immune responses are cytotoxic $CD8^+$ T lymphocytes, which are efficient mediators of viral clearance. Therefore $CD8^+$ T cells would be an appropriate component of a T cell-based vaccine [1] .

Vaccinations aim to induce a long-term immunological memory, which composes of memory B and T cells and antibody secreting plasma cells [2]. However, in the past, the development of vaccines didn't focus on the importance of T cells in providing protection against disease [3]. Instead the protective effect is often achieved by inducing high titers of antibodies that recognize and mark the pathogen for clearance and destruction. Nowadays there is an increased need for understanding the mechanisms of cellular immune memory to be able to develop anti-tumor vaccines or vaccines against chronic pathogens such as HIV or HCV, which rely on the specific killing of infected or transformed cells by cytotoxic $CD8^+$ T cells [4]. The identification of approaches to selectively enrich cytotoxic T cells would be of great benefit. In contrast, the induction of a powerful T cell memory is the major goal in prophylactic vaccinations. So far, most vaccinations fail to induce memory T cells or effector T cells cause severe side effects through the secretion of inflammatory cytokines [5] [6]. Elucidating the mechanisms that lead to the generation of effector or memory T cells would allow to selectively targeting effector or memory T cells. So far, it is still not know if memory precursor T cells, which differentiate into memory T cells develop directly from naïve T cells or via the effector T cell lineage [7]. Until today, markers to distinguish memory precursor T cells from effector T cells in the early phase of a T cell response are missing. Along with the very low numbers of memory precursors, overwhelmed by effector T cells, these cells are difficult to study [8]. Therefore, the identification of the branching point and the underlying mechanism is still a challenge [9] [7] [4]. With the help of the immunosuppressive drug leflunomide, this study yields novel and important insights into the generation of effector and memory T cells that can be used to improve T cell mediated vaccinations.

3.2 CD8$^+$ T cell activation and differentiation

The activation of antigen-specific naïve CD8$^+$ T cells in course of an acute infection or vaccination triggers a series of events, which can be characterized into three different phases: a period of initial T cell activation and expansion, a contraction phase, and the establishment of memory T cells (Figure 1) [10].

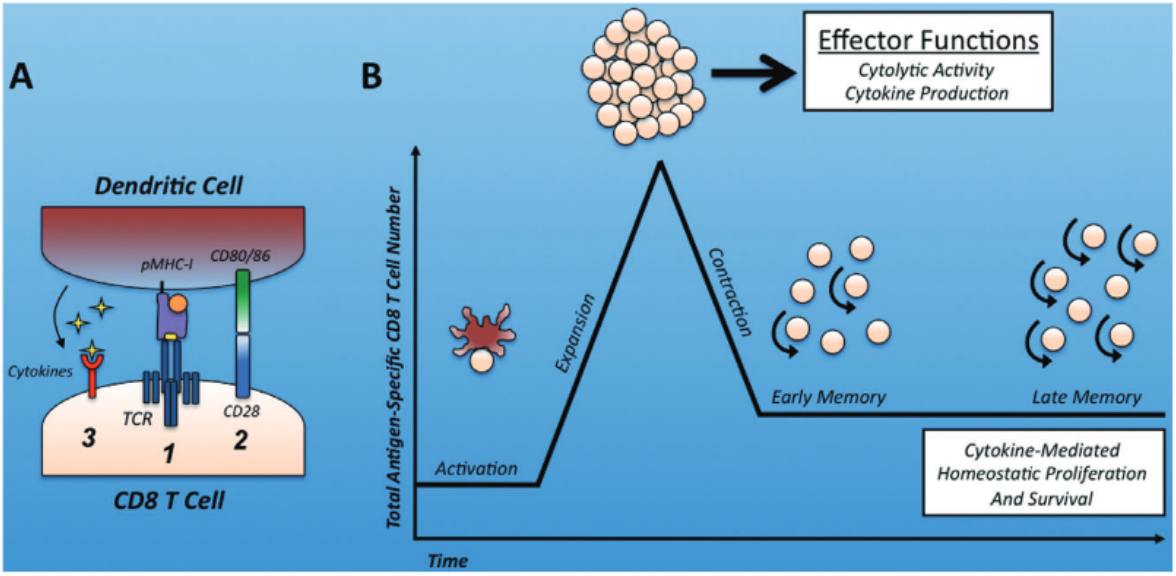

Figure 1. CD8$^+$ T cell activation and differentiation kinetics following an acute infection.

(A) The activation of T cells by DCs requires three different signals: 1. TCR signaling 2. Co-stimulation 3. Cytokines. **(B)** Kinetics of a T cell response in an acute infection. After initial activation of naïve T cells, T cells massively expand and differentiate into effector T cells. During the contraction phase most of the effector T cells die by apoptosis. Only 5-10% of the T cells are able to form long-lived memory T cells [10].

T cell activation

Naive cytotoxic CD8$^+$ T cells continuously migrate between the blood and secondary lymphoid organs such as lymph nodes and spleen in search for a certain (cognate) antigen [10]. Every T cell bears a TCR, which recognizes a limited variety of peptides, bound to major histocompatibility complex class I molecules (pMHC) presented on antigen presenting cells (APC). These APC such as dendritic cells (DC) uptake, process and present the antigens on their surface bound to MHC molecules [11]. The priming of naïve cytotoxic T cells by APCs takes place in secondary lymphoid organs. T cells need three different stimuli to become fully activated: an initial signal

mediated by the stimulation of the T-cell receptor (TCR), a co-stimulatory signal provided by the interaction of molecules between APC and T cell and the secretion of inflammatory cytokines [10] (Figure 1).

Binding of the TCR to a cognate peptide leads to the activation of signaling cascades downstream the TCR, which changes the gene-expression and leads to the proliferation of T cells. To sustain and integrate the TCR signaling co-stimulatory signals are needed. Signal 1 in the absence of co-stimulation by Signal 2 results in T cell anergy or deletion [10]. The third signal provided by inflammatory cytokines has a more fundamental role in regulating responses [12]. Signal 1 and 2 are crucial to initiate the proliferation of naive T cells but the specific cytokine signal leads to the acquisition of normal effector functions, better survival and the generation of memory T cells [12, 13].

Naïve $CD8^+$ T cells interact with APC in three sequential stages. Stage 1 constitutes the first 8h after T cells enter the secondary lymphoid organs and is characterized by a short encounter of the T cell with DCs. In the second stage (8h-24h) T cells and DC form so called T cell-DC conjugates (immunological synapse) that are stable for more than 1 hour. After about 24h T cells express the early activation marker CD69 and the immediate up-regulated gene Nur77. T cell division has not occurred yet. In phase three (24h after homing), T cells dissociate form DCs, proliferate and migrate into the periphery [14].

T cell expansion and differentiation

At the early stage of the infection, only one $CD8^+$ T cell in 10^5 is specific for a cognate antigen in mouse and human [15]. These antigen-specific T cells must greatly expand to combat against the fast replicating pathogen. In a lymphocytic choriomeningitis virus (LCMV) infection, $CD8^+$ T cells divide about 15 times and 16-19 times in a Listeria monocytogenes (Lm) infection [16]. The expansion of $CD8^+$ T cells goes hand in hand with the differentiation of these cells into cytotoxic T cells that kill infected cells through the secretion of granzymes and perforin and secrete cytokines such as IFN-γ and TNF-α [6]. Furthermore, during their differentiation into effector cells, T cells acquire the ability to migrate from lymphoid to non-lymphoid tissues. This is mediated by the down regulation of the expression of lymph node homing receptors such as L-Selectin (CD62L) and the C-C chemokine receptor type

7 (CCR7). In contrast, memory precursor as central memory T cells (T_{CM}) and memory T cells are mainly located to lymphoid organs and express high levels of CD62L [17]. During the proliferation and differentiation T cells up-regulate the marker CD44 [14].

At the peak of the infection, the cell population mainly consists of cytotoxic T cells. However, recent studies could show that these cells are not uniform and can be separated into multiple subsets based on a different gene and protein expression or long-term fate [6]. The heterogeneous populations of effector and memory T cells and their regulation will be discussed in section 3.4 and 3.6.

Contraction and the establishment of T cell memory

Following the elimination of the pathogens most of the effector $CD8^+$ T cells die by apoptosis during the contraction phase. Only 5-10 % of the pathogen-specific cells survive and further differentiate into long-living memory T cells. In acute infections such as Lm or LCMV infections it could be shown that a heterogeneous population of effector $CD8^+$ T cells and memory precursor T cells arise during an infection with a different potential to persist and to form the memory T cell pool [6].

Following the contraction phase, a memory T cell population is formed which is maintained in the absence of antigen [18]. This memory population is maintained at a constant size over a long period of time, which is achieved by a steady division of memory T cells (homeostatic turnover) [19]. This homeostasis is regulated primarily by the cytokines IL-7 and IL-15. IL-7 signals are important for the survival of memory T cells while IL-15 is responsible for the homeostatic divisions. The acquisition of responsiveness to these cytokines is achieved during the transition from effector to memory T cells and is one of the key changes that lead to the differentiation of antigen-independent long-lived memory T cells [20-22].

Until now it is not fully understood how the differentiation of these heterogeneous pool of effector and memory $CD8^+$ T cells is regulated. In section 3.4 some possible models are proposed.

3.3 Model systems to study T cell responses in acute infections

The specific tracking of few numbers of $CD8^+$ T cells and the ability to manipulate the model pathogen provided a powerful tool in understanding $CD8^+$ T cell responses after infections [23]. So far, several model systems exist to study the T cell responses in acute infections.

Listeria monocytogenes

A widely used pathogen that results in the induction of a robust $CD8^+$ T cell response is the intracellular bacterium Listeria monocytogenes (Lm) [23]. Upon infection, the innate immune system is responsible for the early control of the listeria infection. In the spleen this bacterium first localizes within macrophages, which up take this gram-positive bacterial pathogen [24]. Inside the phagosome listeria uses its unique ability to secrets the pore-forming toxin listeriolysin O (LLO) and gains access into the cytosol. Within the cytosol it starts to replicate. To spread from cell to cell, listeria is creating host actin polymers by using the bacterial surface protein actin-assembly-inducing protein (ActA) [23, 25]. Although the innate immune system is important for the initial control of the listeria infection, cytotoxic T cells are needed for final clearance of the intracellular bacteria [24].

LCMV virus

The infection of mice with lymphocytic choriomeningitis virus (LCMV) is a widely used model system to study $CD8^+$ T cell responses [26]. LCMV is a small arenavirus within the Arenaviridae family with a genome that consist of two negative-sense single-stranded RNA segments. The natural occurrence of LCMV is restricted to rodents but a human infection can be triggered by direct contact with infected animals and by inhalation of infectious excrete or secrete [27]. During the course of an acute LCMV infection the $CD8^+$ T cell response is directed against two epitopes derived from the glycoprotein (amino acids 33-41) and the nucleoprotein (amino acids 396-404), as well as several other epitopes [27, 28]. LCMV can cause an acute or chronic infection dependent on the strain that was used. While LCMVArmstrong and WE strain lead to an acute infection, the clone 13 or docile strain will cause a chronic infection in mice [29].

VSV virus

The Vesicular Stomatitis Virus (VSV) is a cytopathic negative-strand RNA virus of the Rhabdoviridae family. It replicates rapidly and viral expressed proteins are readily presented which generates a strong $CD8^+$ T cell response [30]. The natural hosts of this virus are cattle, rodents, swine and horses [31]. Recombinant VSVs expressing foreign proteins have been studied as vaccine vectors for influenza virus or Ebola virus and recent studies raveled VSV as a promising oncolytic agent [31, 32].

Transgenic T cells: P14 and OT-1 T cells

Endogenous $CD8^+$ T cell responses are not always easy to detect due to the low number of antigen- specific T cells. To overcome this limitation, TCR transgenic T cells can be used. TCR transgenic cells express a transgene for α and β chain of a T cell receptor that is specific for a peptide/MHC complex. The transfer of these T cells allows investigating a T cell response with a defined affinity between the TCR and the peptide/MHC complex. Moreover, the transfer of a defined amount of TCR transgenic T cells makes it easier to visualize the $CD8^+$ T cell response. Today, several pathogens have been manipulated to express a certain antigen for which TCR transgenic T cells exist [33].

P14 T cells express a $CD8^+$ TCR, which recognizes the gp33-41 epitope KAVYNFATC derived from the LCMV glycoprotein in context of the MHC class I molecule H-2Db. OT-1 T cells express a TCR which recognizes the chicken Ovalbumin (Ova) derived SIINFEKL epitope presented on MHC class 1 (H-2Kb).

P14 and OT-1 T cells are crossed to different congenic markers (CD45.1, CD45.2, CD90.1, CD90.2), which allows the adoptive transfer and *in vivo* tracking of different T cell populations [34].

3.4 Effector versus memory T cell differentiation: proposed models

The fate decision of activated T cells could be taken before the first cell division or at a later stage. Therefore, several model exist that predict the effector and memory T cell differentiation (Figure 2).

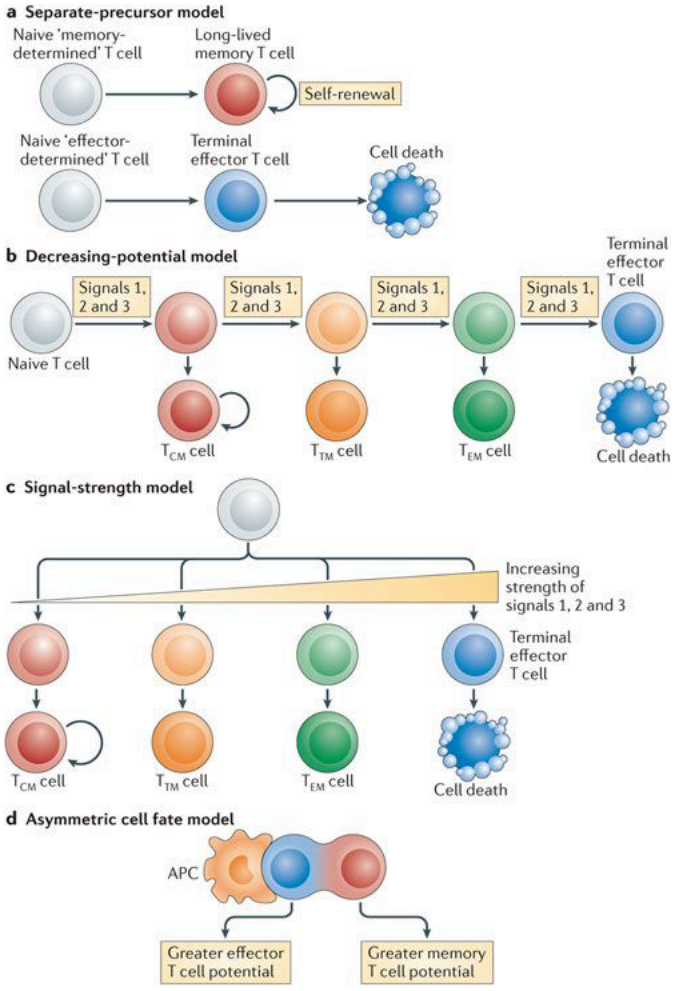

Figure 2. Different proposed models to generate heterogeneous pools of effector- and memory CD8$^+$ T cells.

In these models, the potential of T cells to differentiate into effector or memory T cells is specified in an early stage of the T cell activation (Separate precursor (**a**) or asymmetric cell fate model (**d**)) or in a later stage (Decreasing potential (**b**) or signal- strength model (**c**)) of the T cell response [6].

Separate- precursor model

Using new technologies such as the adoptive transfer of single cells or barcode labeled T cells it could recently been shown that one naïve T cells is able to differentiate in both effector and memory T cells [35, 36] (Figure 2a). By comparing the barcodes of differentiated effector and memory T cells in different acute infections, at different anatomic sites and different TCR avidities, Gerlach et al. could show that naïve T cells have effector and memory progeny and the T cell fate is not determined by the priming APC or the time of T cell priming [36]. Nevertheless, it is important to consider that both studies where carried out by using TCR transgenic T cells with the same affinity for the antigen. Therefore, the potential effects of the TCR strength on the T cell fate are not included [6].

Decreasing- potential model

This model predicts that activated T cells, which receive a repetitive stimulation with antigens and inflammation after the priming phase will differentiate towards the effector T cell lineage (Figure 2b). Descendants that do not encounter further antigen stimulation will loose the effector functions such as cytolytic capacity and differentiate into long-lived memory T cells. If inflammatory signals and antigenic stimulation is prolonged T cells mainly develop into effector T cells whereas shortening the antigen exposure and decreasing the inflammation leads to memory T cell formation [6, 9, 37].

Signal- strength model

This model focuses on the overall strength of signals, which a T cell receives during the early T cell activation phase (Figure 2c). The signals are defined as antigen stimulation (signal 1), co-stimulation (signal 2) and pro-inflammatory cytokines (3). It is thought that a strong stimulation selects out T cells with a potential to form memory T cells. In contrast, very strong signals can cause a terminal effector T cell differentiation. The intensity of the signals, which a T cell receives, specifies the T cell fate [6].

Asymmetric cell fate model

This model relies on the determining role of the priming APC and suggests that effector and memory T cells can arise from the same naïve T cells through asymmetric cell division (Figure 2d). This occurs before the first T cell division and is determined by the localization of the activated T cell to the APC. A daughter cell localized proximal to the APC is more likely to differentiate into a effector T cell while the distal daughter cell will likely develop into a memory T cell [6, 36]. It is thought, that the T cell with its proximity to the APC receives stronger TCR and co-stimulatory signals and therefore differentiates into an effector T cell. Chang et al. could demonstrate that the first two daughter cells are phenotypically and functionally differentiated towards the effector or memory lineage [38].

3.5 Receptors and transcription factors that determine effector and memory T cells

At the peak of the infection the pool of pathogen-specific T cells is heterogeneous and enriched for effector and memory precursor T cells, which can be divided in several subsets based on differences in protein and gene expression [6].

KLRG1 and IL7 receptor α

At day 7 post infection a subset of antigen-specific $CD8^+$ T cells upregulate or retain the IL7 receptor α (CD127) expression and differentiate into long-lived memory T cells [20]. The expression of killer-cell lectin-like receptor G1 (KLRG1) is further used to distinguish the memory and effector T cell population. Based on the expression of KLRG1 and CD127 antigen-specific $CD8^+$ T cells can be separated in $KLRG1^{high}$ $CD127^{low}$ short lived effector T cells (SLEC) and $KLRG1^{low}$ $CD127^{high}$ memory precursor T cells [5, 20]. At the peak of the acute infection $KLRG1^{low}$ $CD127^{high}$ $CD8^+$ T cells, which constitute 5 to 10% of the cell population, preferentially survive. These cells differentiate from T cells with an activated phenotype, high levels of granzyme B, and low levels of Bcl-2 into memory $CD8^+$ T cells characterized by a resting phenotype, low granzyme B expression, and high levels of Bcl-2 [20]. In contrast, $KLRG1^{high}$ $CD127^{low}$ effector CD8+ T cells die during the T cell contraction phase [6]. Although these two receptors are widely used to distinguish effector and memory

$CD8^+$ T cells, recent studies could show that T cell subsets with intermediate differentiation states could be identified [39]. Furthermore, there are some interconversions between these subsets. Herndler-Brandstetter et al. could show that $KLRG1^+$ effector $CD8^+$ T cells at d6 post infection lose the KLRG1 expression and differentiate into memory T cells [40].
Due to the identification of new cell surface markers, the memory T cell population at the peak of the infection can be further divided into different subsets. This will be discussed in the following section.

Beside the identification of effector or memory specific cell surface proteins, the transcriptional circuit that underlies their differentiation process has started to be investigated. One of the most studied transcription factors that regulate the effector and memory T cell differentiation are the T-box transcription factors T-bet and Eomesodermin (Eomes) [6].

T-bet and Eomes

The T-bet expression is induced by TCR signaling and further amplified by the inflammatory cytokine IL-12 and mTOR signaling [6]. Joshi et al. could show that the amount of inflammatory cytokines present during the T cell priming regulates the effector versus memory T cell differentiation [9]. A high amount of inflammation leads to a high T-bet expression, which induces the differentiation of short-lived effector T cells (SLECs). Furthermore, a lack of the T-bet expression impairs the differentiation of terminal effector T cells and promotes the differentiation of memory T cells, but when overexpressed, T-bet is sufficient to rescue the effector T cell formation.

The expression of Eomes promotes the differentiation of memory T cells. $CD8^+$ T cells deficient in Eomes are able to differentiate into memory precursor T cells but are unable to form long-lived memory T cells. Moreover, $CD8^+$ T cells lacking Eomes contain fewer T_{CM} cells [41]. The expression of Eomes is induced subsequently to that of T-bet but in a Runx3 dependent manner. It is further amplified by IL-2 and Wnt signaling and the expression of Tcf1 but repressed by IL-12 and mTOR signaling [6]. The Eomes expression increases from the effector to memory phase, whereas the T-bet expression is highest in early effector T cells and starts to decline afterwards [42]. Therefore, it seems that the T-bet and Eomes expression is reciprocally regulated.

Thus, the ratio of T-bet to Eomes seems to determine the fate of antigen-specific $CD8^+$ T cells [6, 42].

Tcf1

Tcf1 is a transcription factor of the canonical Wingless/Integration 1 (Wnt) signaling pathway. It is encoded by the Tcf7 locus and implicated in the T lymphocyte lineage specification during T cell development. Recent publications could also demonstrate a peripheral role of Tcf1 in the effector and memory T cell differentiation [43, 44]. Mice lacking Tcf1 mount a normal effector $CD8^+$ T cell response in an acute infection but showed a reduced magnitude of T cell proliferation [45, 46]. Furthermore, *Tcf7*$^{-/-}$ memory $CD8^+$ T cells in secondary lymphoid organs underwent a progressive loss over time due to a diminished responsiveness to IL-15 [46]. The T-box transcription factors T-bet and Eomes are implicated in the IL-15 responsiveness of $CD8^+$ memory T cells [47]. An diminished Eomes expression was observed in *Tcf7*$^{-/-}$ memory T cells and further experiments revealed the direct regulation of Eomes expression by the Wnt/Tcf1 pathway [46]. A further characterization of the phenotype of *Tcf7*$^{-/-}$ memory $CD8^+$ T cells showed that *Tcf7*$^{-/-}$ T cells exhibit a T_{EM} phenotype whereas T_{CM} are missing. This indicates an essential role of Tcf1 in the differentiation of T_{CM} cells [46]. Furthermore, the secondary re- expansion of memory T cells, which is a hallmark of T_{CM} cells was impaired in *Tcf7*$^{-/-}$ $CD8^+$ T cells [45].

Blimp-1

The B lymphocyte-induced maturation protein 1 (Blimp-1) is a SET domain and a zinc finger–containing transcriptional repressor encoded by the *Prdm-1* gene. It has been shown to be important for the plasma cell differentiation [48]. Furthermore, it could been recently shown that Blimp-1 is essential for the differentiation of effector $CD8^+$ T cells and an efficient memory recall response [49]. $CD8^+$ T cells deficient in Blimp-1 fail to regulate the transcriptional program, which is crucial for an effective cytotoxic T cell response and primarily develop into memory precursor cells. These results reveal a critical role for Blimp-1 in controlling the effector $CD8^+$ differentiation. Blimp-1 is needed to suppress the program that leads to the development of memory T cell in pathogen-specific $CD8^+$ T cells [49, 50]. IL-2 and other cytokines induce Blimp-1 expression in $CD8^+$ T cells during the clonal expansion, but its expression gradually declines during the effector to memory transition phase. Blimp-1 further

suppresses the IL-2 gene transcription, thereby serves as a negative feedback loop to alter T cell gene expression [48, 50, 51].

Id2 and Id3

Inhibitor of DNA binding 2 (ID2) and ID3 are both expressed by effector $CD8^+$ T cells and negatively regulate the DNA-binding activity of E-protein transcription factors [6, 52]. The activities of Id2 and Id3 are dose and time dependent regulated. Id2 is needed for the survival of effector $CD8^+$ T cells during the naive to effector T cell transition [53, 54, 6]. To maintain effector $CD8^+$ T cells a continued Id2 regulation of E-protein activity is required [55]. Id2 is essential for the induction of high levels of *Tbx21*. A loss of Id2 expression in $CD8^+$ T cells impairs the effector T cell differentiation and program T cells to adopt a memory cell phenotype with increased *Eomes* and *Tcf7* expression [53].

ID3 is critical for the survival of effector T cells during the effector to memory cell transition [6]. It is known that signaling through the T cell antigen receptor (TCR) and TGF-β can influence Id3 expression. The Id3 gene expression is furthermore directly regulated by E-protein transcription factors and Blimp-1. A loss in Id3 expression leads to a defective memory T cell formation [56].

3.6 Memory T cell subsets: T_{CM}, T_{EM} and T_{RM}

Memory $CD8^+$ T cells consist of a heterogeneous population of T cells, which can be classified in at least two phenotypically and functionally distinct subsets: effector memory (T_{EM}) and central memory (T_{CM}) T cells [6, 57]. Memory T cells that express CD62L and CCR7, which allow the homing to lymph nodes, are termed central memory T cells. $CD62L^{neg}$ $CCR7^{neg}$ memory T cells are referred as effector memory cells. The differential expression of the marker CD27 further allows distinguishing T_{EM} and T_{CM} cells. T_{CM} cells are mostly $CD27^{hi}$, whereas T_{EM} cells are $CD27^{lo/int.}$ [6, 57, 58].

T_{CM} and T_{EM} cells are further different in their anatomical location and function. While T_{CM} cells migrate through secondary lymphoid organs, T_{EM} cells are located in peripheral tissues. Functionally, T_{CM} cells are able to mount a more robust recall response and produce interleukin-2 (IL-2), whereas $CD8^+$ T_{EM} cells are immediate producers of cytotoxic proteins [57, 58]. During acute viral or bacterial infections, T_{CM}

cells mediated an enhanced protection, which was due to their inherent proliferative advantage over T_{EM} following antigenic stimulation and not to better effector functions [57]. Different transcriptional regulators regulate the differentiation of T_{CM} and T_{EM} cells. T_{CM} formation is favored by increased expression of Bcl-6 and inactivation of T-bet, Blimp-1, and Id2 [54, 59] [49]. So far, it is still not revealed how T_{EM} and T_{CM} cells arise. Wherry et al. propose that T_{CM} and T_{EM} cells are part of a continuum that ends with the development of T_{CM} cells. T_{EM} cells are an „intermediate“ cell population whereas T_{CM} cells are the “true” memory cells due to their long-term persistence *in vivo* and the ability to rapidly expand in a secondary infection. Furthermore, they could show that the conversion rate is programmed during the initial period of encounter with antigen *in vivo* [57].

Several recent publications showed that other memory T cells exist which reside long-term in the brain and mucosal tissue with limited levels of recirculation. These cells are termed as tissue resident T cells (T_{RM}) and can be identified by expression of the markers CD103 and CD69 and a low expression of CD27. T_{RM} cells, similar T_{EM} cells, mediate immediate effector functions and a first-line defense at the pathogen entry site [60, 61]. So far, it is still unknown when T_{RM} cells branch off during the T cell response.

3.7 Metabolic regulation of T cell differentiation

T cell activation induced by TCR ligation and binding of co-stimulatory molecules leads to a transition of quiescent naïve T cells into activated, highly proliferating T cells [64]. The proliferation and subsequent production of effector molecules are accompanied by substantial changes in the T cell metabolism (Figure 3) [62].

Naïve T cells primarily generate ATP through mitochondrial oxidative phosphorylation (OXPHOS) and fatty acid oxidation (FAO). To meet their energy demand activated T cells preferentially use aerobic glycolysis over OXPHOS, consuming massive amounts of glucose, which enables to generate effector functions. Furthermore activated T cells increase lipid synthesis and glutaminolysis to fuel the rapid cell growth and proliferation [63, 69]. Although OXPHOS is more efficient in the generation of ATP molecules, aerobic glycolysis generates different metabolic intermediates, which are for example used in the de novo synthesis of nucleotides.

After the clearance of the antigen, effector T cells reset back to OXPHOS and FAO and differentiate into long-lived memory T cells [6, 62, 64] (Figure 3).

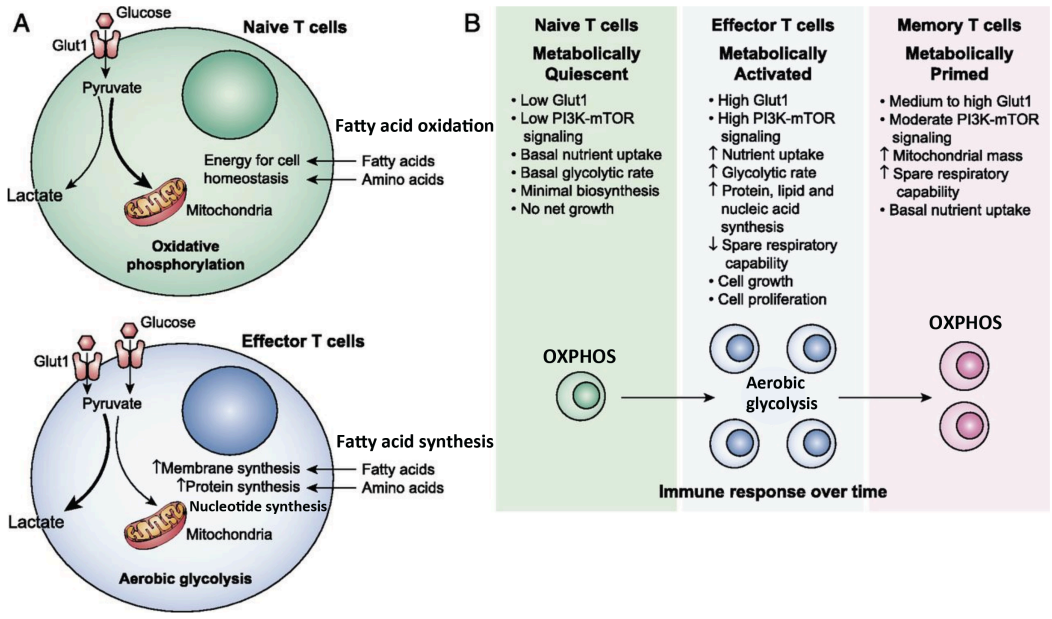

Figure 3. Metabolic shifts during the immune response

Naïve T cells (green) are metabolically quiescent and oxidize pyruvate or fatty acids to produce reducing equivalents to generate ATP via OXPHOS. To meet biosynthetic requirements in activated T cells, fatty acid oxidation is inhibited while glycolysis, fatty acid and nucleotide synthesis increases. Intermediates from glycolysis, lipid synthesis and glutamine oxidation provide substrates to fuel the rapid cell growth and proliferation of activated T cells. At the end of an immune response, the cells that survive during the contraction phase become memory T cells, which use lipid oxidation and OXPHOS to meet their energy demands. Modified from [65].

Glycolysis, tricarboxylic acid cycle (TCA) and oxidative phosphorylation (OXPHOS)

ATP can be derived from glucose through two integrated pathways: Glycolysis and TCA cycle [64]. Upon encounter with an antigen, TCR signaling leads to the up regulation of glucose (Glut1) and amino acid transporters on the surface of activated T cells (Figure 3). After being imported glucose is metabolized in several cytosolic enzymatic reactions to pyruvate with a net production of two ATP molecules [63, 66] (Figure 4, green). In activated T cells pyruvate is converted to lactate in the cytosol by the enzyme lactate dehydrogenase (LDH). This regenerates NAD^+, which is required as a cofactor to engage glycolytic reactions. The transformation of pyruvate

into lactate in presence of oxygen is known as Warburg effect (or aerobic glycolysis) and has been first observed in tumor cells [67]. So far it is still not fully understood why activated T cells with an increased demand for energy use such an insufficient process to generate ATP. It has been recently shown that the intermediate metabolites of glycolysis are used to generate nucleotides (Pentose phosphate pathway (Figure 4, dark blue), serine biosynthesis pathway (Figure 4, red) and amino acids which are important to meet the metabolic demands of proliferating T cells [63]. Furthermore, the glycolytic reactions are important for the cytotoxic effector functions of T cells, the de novo fatty acid biosynthesis (FAS) (Figure 4, light blue) and a better maintenance of redox balance [63, 68].

Alternatively, the TCA cycle in the mitochondria is the second pathway where pyruvate is decarboxylated to Acetyl- CoA (Figure 4, orange). Each cycle of oxidation through several enzymatic reactions generates 4 NADH and 1 FADH2 molecules [64]. Resting and memory T cells completely oxidize pyruvate via the TCA cycle thereby generating NADH and FADH2. Inside the mitochondria, NADH and FADH2 are converted to 36 molecules ATP per glucose molecule by the electron transport chain (ETC) [67]. The ETC is located in the inner mitochondrial membrane and consists of four electron carriers organized into four complexes. A fifth transmembrane protein, the ATP synthase couples the generated energy to ATP synthesis [67] (Figure 4, brown). Complex 1 oxidizes NADH to NAD^+. The electrons are transferred to Coenzyme Q (Ubiquinone), which carries electrons through the membrane to complex 3. Complex 2 oxidizes FADH2 to FAD and donates the electrons to Coenzyme Q and then to complex 3. In complex 3 electrons are transferred from cytochrome b to cytochrome c. Finally, the electrons are transferred to complex 4, where they are transmitted to molecular oxygen thereby generating water. The transfer of electrons is accompanied with the transfer of protons to the intermembrane space. This generates a different electric gradient between both sides of the membrane, which is resolved by the fifth complex of the ETC, the ATP synthase. This protein pumps the protons back to the mitochondrial matrix, which leads to the phosphorylation of ADP to ATP. This process is called oxidative phosphorylation [67].

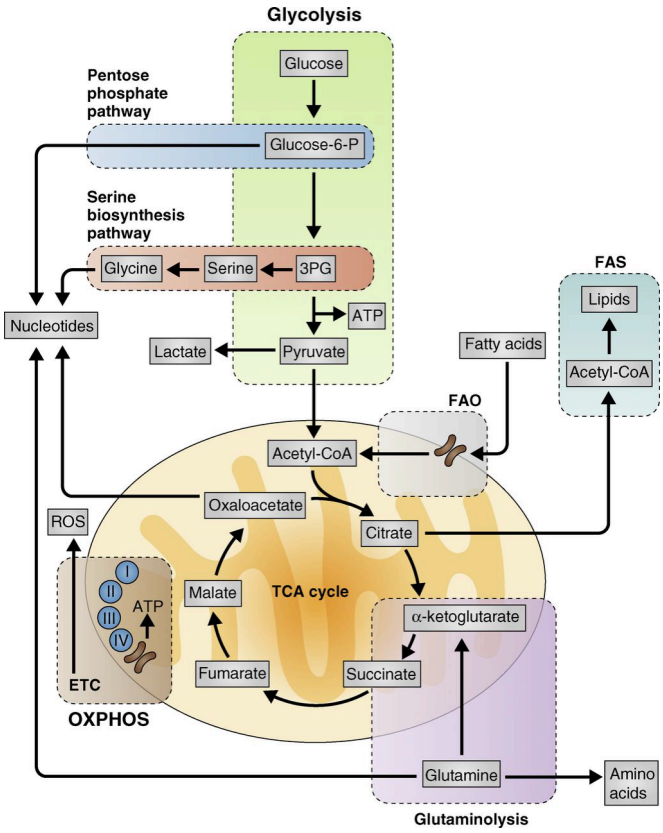

Figure 4. Metabolic pathways in T cells

ATP can be generated from glucose through two integrated metabolic pathways. In the glycolysis (green), glucose is enzymatically converted into pyruvate. Afterwards, pyruvate gets further metabolized to acetyl-CoA. The breakdown of Acetyl-CoA inside the TCA cycle (orange) through several enzymatic reactions leads to the generation of reducing equivalents to fuel OXPHOS (brown). Beside Glucose, substrates like glutamine or fatty acids can further be metabolized via glutaminolysis (purple) or fatty acid oxidation (FAO, grey) in the TCA cycle. To meet the increased demand in nucleotides, intermediates generated in the glycolysis can be used for the de novo synthesis of nucleotides via the pentose phosphate (dark blue) and serine biosynthesis pathway (red). Furthermore, glutamine can be used to generate precursors for amino acid and nucleotide synthesis. To synthesis lipids, citrate from the TCA cycle can be converted to acetyl-CoA, which is further converted to build up fatty acids [64].

Glutaminolysis

Another important substrate for activated T cells is glutamine. After their activation T cells increase the expression of glutamine transporters like Slc7a5 [64]. To meet the increased demand for biosynthetic precursors and NADPH, glutamine supports the TCA cycle through conversion of glutamate via glutaminases. Glutamate is further converted to alpha-ketoglutarate (α-KG) [63]. Furthermore, glutamine can be used to generate precursors for amino acid and nucleotide biosynthesis (Figure 4, purple*). In vitro* studies could underline the importance of glutamine for T cells. The activation of T cells and subsequent proliferation was inhibited if glutamine and glucose was limited in the media [8]. Unlike activated T cells, naïve and memory T cells do not proliferate and have low metabolic requirements. These cells make use of fatty acids

and pyruvate oxidation via the TCA cycle to meet their energy demand (Figure 3) [67].

Fatty acid oxidation (FAO) and spare respiratory capacity (SRC)

Fatty acid oxidation mainly occurs in the mitochondria. Inside the mitochondria enzymatic reactions shorten long-chain fatty acids to acetyl-CoA (Figure 4, grey) [64]. These fatty acid- derived Acetyl-CoA molecules will enter the TCA cycle. NADH and FADH2, which was generated during the enzymatic reactions, can be further used as electron donors in the ETC [67]. Memory T cells are not only dependent on FAO to fuel their metabolic demands but also for their long-term persistence and the ability to robustly respond to antigen stimulation. During the immune response, the cytokines IL-7 and IL-15 promote FAO in T cells. As a result, memory T cells display an increased mitochondrial mass and thus a greater mitochondrial spare respiratory capacity (SRC) (Figure 3) [64]. SRC is defined as the maximal mitochondrial respiratory capacity available to a cell to produce energy under conditions of increased stress [63]. This gives memory T cells an advantage compared to naïve and effector T cells to survive and mount a rapid recall response [64].

Fatty acid synthesis (FAS)

Beside glucose and glutamine, lipids can further support T cell proliferation [67]. They represent a good source for energetic and biosynthetic precursors [63]. After T cell division, the cell membrane of the daughter cell is as twice as large as the original T cell. Therefore, the demand of lipids rapidly increases [67]. 24h after activation *in vitro*, naïve T cells switch from fatty acid oxidation (FAO) to fatty acid synthesis (FAS) [64]. FAS takes place in the cytosol and involves two enzymes, acetyl-CoA carboxylase (ACC) and fatty acid synthase (FASN). ACC carboxylates acetyl-CoA to form malonyl-CoA, which is further converted by FASN to long-chain fatty acids. In an NADPH dependent manner, further acetyl molecules are attached by FASN to generate palmitate. Palmitate can then be used as a precursor to generate other fatty acids [67].

Pentose Phosphate Pathway (PPP) and nucleotide synthesis

The pentose phosphate pathway is important for activated highly proliferating cells as it generates precursors of pentose phosphates required for the synthesis of ribonucleotides [69]. Furthermore, it provides NADPH, which is required to sustain the lipid synthesis [70]. The PPP branches from glycolysis at the first step of glucose metabolism and consists of two different branches: the oxidative branch and the non-oxidative branch.

In the irreversible oxidative branch, glucose-6-phosphate is metabolized to ribulose-5-phosphate by oxidative decarboxylation and NADPH is generated. The non-oxidative branch is reversible and consists of a series of reactions in which phosphorylated sugars are interconverted to generate glycolytic intermediates such as fructose-6-phosphate, ribulose-5-phosphate or ribose-5 phosphate. All of these intermediates can be converted into pentose phosphates. Ribose- 5- phosphate is further processed into phosphoribosyl pyrophosphate (PRPP), which is used in the de novo synthesis of purine and pyrimidine nucleotides [70, 71]. The de novo synthesis of pyrimidines is described in section 3.8.

3.8 Leflunomide: a drug with the potential to block the effector T cell differentiation

In this study we explored the impact of leflunomide on the effector and memory T cell differentiation. This was based on preliminary data that indicated a critical impact. Therefore, common knowledge of leflunomide is reviewed in this introduction.

Leflunomide is commonly used in the treatment of rheumatoid arthritis (RA) and multiple sclerosis (MS) [72-76] but several recent publications also revealed its promising anti-tumor potential [72, 77, 78]. Leflunomide was identified from a series of compounds planned as agricultural pesticides by scientists at Hoechst Research Laboratories [79]. Bartlett et al. realized the clinical potential of this drug in 1991. Today, leflunomide is approved in the US and EU and in 43 other states all over the world for the treatment of RA and its immunosuppressive function is used primarily to target activated lymphocytes [80, 81, 82].

Pharmacokinetic properties

Orally administered, the first metabolic step of leflunomide takes place in the gastrointestinal tract where it gets metabolized into its active metabolite A77 1726 (teriflunomide) (Figure 5). The second metabolic step takes place in the liver and plasma. At the end, leflunomide is almost completely metabolized to the active metabolite teriflunomide and to minor extend to TFMA (4-trifluoromethylanilline) [80]. After oral administration the peak plasma concentration occurs after 5-24 hours in humans and the plasma half-life is approximately 15 days due to the high level of protein binding (> 99,3%) [83]. At the present time no specific enzyme has been identified as the primary route of metabolism for leflunomide. *In vivo* and *in vitro* studies suggest a role for the gut intestinal wall and the liver in drug metabolism. Furthermore, *in vitro* interaction studies show a role of cytochrome P450 but *in vivo* this enzyme is only involved to a small extent [83]. To reach a steady state condition leflunomide has to be administrated in repeated loading doses. If administrated one time, 90 % of the leflunomide gets eliminated in urine or feces. A loading dose of 100 mg for 3 days is used to rapidly reach the steady-state levels. Without a loading dose, it would require 4-8 weeks of dosing [74]. After 3 days, humans receive a maintenance dose of 20 mg leflunomide every day [84]. The active metabolite teriflunomide is eliminated by further metabolism in two routes [82]. In the first 96 hours' renal elimination was more significant after which fecal elimination was predominantly used. Analysis of collected urinary and fecal samples revealed that the primary urinary metabolites are the leflunomide glucuronides and an oxanilic acid derivate of teriflunomide [82]. The primary fecal metabolite was teriflunomide. Unchanged leflunomide could not be detected. After the leflunomide treatment was stopped in humans it takes about 8 months to 2 years to remove the teriflunomide from their plasma. To accelerate the removal oral administration of charcoal (8g three times daily) or cholestyramine (50g four times a day) is used. Both treatments reduce the half live of teriflunomide to approximately 1 to 2 days [82].

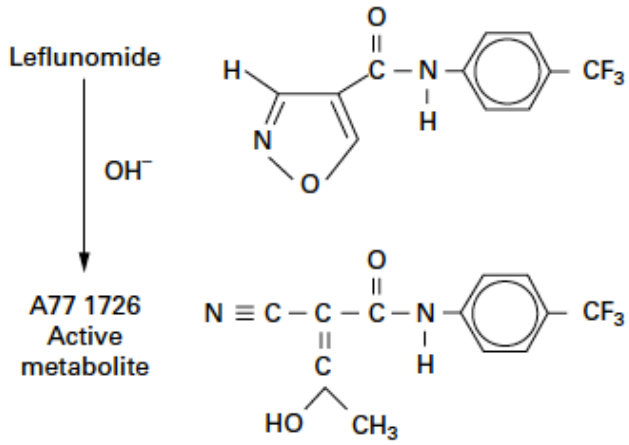

Figure 5: Chemical structure and metabolism of leflunomide

The biotransformation pathway of leflunomide involves an N–O bond cleavage on its isoxazole ring, which leads to the formation of the 2-cyano-3-oxo-[(4trifluoromethyl)phenyl]butyramide (A771726; teriflunomide) metabolite [85].

Mode of action

So far, *in vitro* and *in vivo* studies could show that teriflunomide prevents the expansion of activated lymphocytes by interfering with the cell cycle progression [80]. Until today two possible mechanisms have been suggested how teriflunomide could act on lymphocytes [85]:

1. The inhibition of the de novo pyrimidine synthesis via blocking of the dihydro-orotate dehydrogenase (DHODH) in the G1 Phase of the cell cycle.
2. The inhibition of tyrosine kinases associated with the signal transduction cascade in the Go phase of the cell cycle.

The immunomodulatory effect of teriflunomide occurs at doses that inhibits DHODH but not tyrosine kinases. Therefore, at present, the postulated mode of action of A771726 relies on the inhibition of the enzymatic activity of DHODH and the associated block in the de novo pyrimidine synthesis. At higher administration leflunomide seems also to interfere with the tyrosine phosphorylation [83, 85].

1. De novo pyrimidine synthesis

Purine and pyrimidine nucleotides play critical roles in DNA and RNA synthesis and are therefore required for the proliferation of T cells [86]. Pyrimidine ribonucleotides can derive either from de novo synthesis pathways (Figure 6, blue and green) or from the salvage pathway (Figure 6, red) [87]. If the required substrates are available lymphocytes can use the salvage pathway to maintain the basal homeostatic

requirements for pyrimidine ribonucleotide synthesis by reutilization of previously synthesized pyrimidine rings. After the activation lymphocytes need to expand their pyrimidine pool by roughly eight fold therefore both pathways are utilized to supply the increased demand [85].

The pathway for the de novo synthesis of pyrimidines is induced in the mid G1 phase and leads to the induction of the trifunctional enzyme CAD (carbamoyl-phosphate synthetase 2, aspartate transcarbamylase, and dihydroorotase) (Figure 6, blue). CAD uses an equivalent of L-glutamine, aspartate, and bicarbonate and two equivalents of ATP to make dihydroorotate (DHO) [87]. The FMN-containing enzyme dihydroorotate dehydrogenase (DHODH), located in the inner mitochondria membrane in mammals, reduces DHO to orotic acid while transferring $2e^-$ to Coenzyme Q (Ubiquinone). Due to its location it also connects the de novo pyrimidine synthesis with the electron transport chain of aerobic respiration [88]. The enzyme uridine monophosphate synthetase (UMPS) converts oorotic acid into uridine monophosphate (UMP). Phospho-a-D-ribosyl-1-pyrophosphate (PRPP), derived from the pentose phosphate pathway (section 3.7), is used as a co-substrate. UMP is converted to UDP by cytidine monophosphate kinase (CMPK). UDP can be further converted in the de novo pyrimidine pathway (Figure 6, blue) to UTP by the enzyme nucleoside-diphosphate kinase (NDPK). Furthermore, UDP or CDP are deoxygenated in the pyrimidine deoxyribonucleotide synthesis (Figure 6, green) into deoxy-UDP (dUDP) and dCDP, respectively, by ribonucleotide reductase (RNR). UTP is further converted into CTP by CTP synthetase (CTPS) while dUDP and dCDP are converted to dUTP and dCTP. All these pyrimidine ribonucleotides (CTP, UTP) and deoxyribonucleotides (dCTP, dTTP) are used for RNA and DNA biosynthesis, respectively [87].

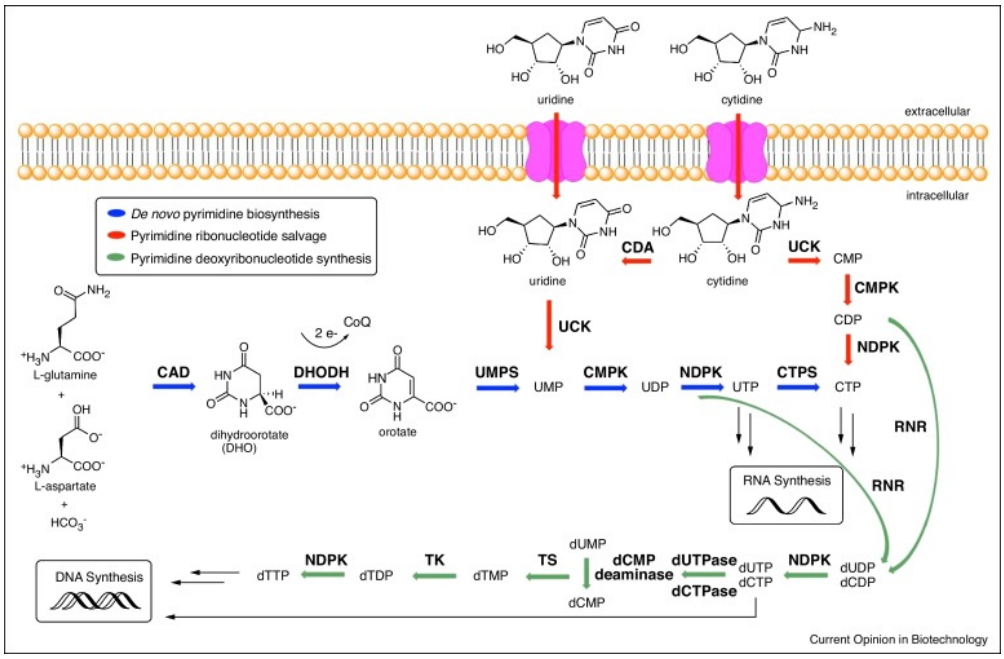

Figure 6. Pathway for the de novo synthesis of pyrimidines.
Pyrimidine ribonucleotides can derive either from de novo synthesis pathways (blue and green) or from the salvage pathway (red) [87].

The immunomodulatory effect of teriflunomide is mediated through the reduction of the activity of the fourth enzyme in the de novo pyrimidine synthesis- dihydroorotase dehydrogenase (DHODH) [83]. In several in vitro studies the inhibitory effect of DHODH has been confirmed and DHODH was shown to be the only enzyme to be inhibited at a therapeutically drug level (Ki 179 nM) [83, 85]. DHODH consist of two binding sites, one for the oxidation of dihydroorotate and one for quinone binding and electron transfer [89]. In a study analyzing the kinetics of DHODH inhibition, it was found that teriflunomide acted as a competitive inhibitor of the ubiquinone binding site and a non-competitive inhibitor of the dihydroorotate binding site [85]. By addition of the pyrimidine uridine *in vitro* the anti-proliferative effect of teriflunomide on T- and B cells can be reversed while the pyridine nucleotides adenine and guanosine have no effect [80, 90]. In addition it has been shown that A77 1726 stimulated murine T cells decrease their UTP levels (95%) and CTP levels (85%) significantly while ATP and GTP levels stay normal [85].

If cytoplasmic pyrimidine levels inside the cell get lower, the sensor protein p53 activates genes involved in cell cycle arrest, induction of apoptosis or DNA repair.

The apoptotic pathway is supposed to be less important as A77 1726 treated lymphocytes exhibit a cytostatic rather than apoptotic defect [83].
Until today, leflunomide was shown to not only interfere with the proliferation of mitogen stimulated T cells *in vitro*. The restriction of de novo pyrimidine biosynthesis was shown to further modulate the Th1 cell and Th2 cell differentiation [91, 92].
Furthermore, DHODH inactivation reduces leukemic cell burden and inhibits melanoma cell proliferation [93-95].

2. The inhibition of tyrosine kinase signaling

The full activation of T cells requires three different signals to proceed from the resting G0 phase to the G1 phase. The first signal is provided through the ligation of the T cell receptor (TCR) complex, which leads to the phosphorylation and activation of protein tyrosine kinases [10]. In *in vitro* studies teriflunomide has been reported to inhibit the phosphorylation of tyrosine kinases [96-98].
Experiments on Jurkat T cells show an impaired phosphorylation of the Src related tyrosine kinases p56lck and p59fyn. Both kinases are associated with the ζ chain of the TCR and after activation they are important to recruit Zap70 to the receptor [98].
Teriflunomide also inhibits the activation of the phospholipase C isozyme γ1, involved in the mobilization of Ca^{2+} *in vitro*. Free Ca^{2+} leads to the dephosphorylation of NF-AT and its translocation into the nucleus where it activates the transcription of IL-2, IL-4 and other cytokines in association with AP-1 [91, 99]. Some results also suggest a suppressive action of teriflunomide on the IL-2 production and the IL-2Rα (CD25) expression on stimulated T cells *in vitro*. The binding of IL-2 to its receptor leads to the activation of the JAK/STAT pathway [100]. It has been shown that A77 1726 suppresses the phosphorylation of JAK1 and JAK3 kinases and the activation of STAT5 [96, 101]. Peripheral T cells from mice deficient in STAT5α and STAT5β are unable to proliferate after engagement of the TCR even in the addition of IL-2. Since teriflunomide inhibits the phosphorylation of STAT5 it is supposed that this could correlate with the anti-proliferative activity of the agent [91]. The tumor necrosis factor-alpha (TNF-α) is involved in pathological immune responses and the effect of leflunomide on TNF-α has been investigated as well. It seems that teriflunomide is a potent inhibitor of TNF-α mediated activation of NF-κB by suppressing the activation of the IKK-β kinase [102].

4. Aim of study

Leflunomide is an immunosuppressive drug frequently used to treat autoimmune diseases such as rheumatoid arthritis and multiple sclerosis. *In vitro*, leflunomide was shown to cause a proliferation arrest of activated lymphocytes by interfering with dihydroorotate dehydrogenase (DHODH) – an essential enzyme in the *de novo* pyrimidine synthesis pathway. However, surprisingly little is known about how leflunomide impacts T cell responses *in vivo*. What raised our interested to investigate the impact of leflunomide on the T cell differentiation *in vivo* was that auto-reactive T cells are sufficiently suppressed in leflunomide treated patients without severely impairing anti-pathogen T cell responses. So far, the mechanism underlying this selective repression remains largely unknown. While monitoring the T cell response in an acute infection we found that the expansion of antigen- specific T cells during the acute phase was massively diminished in leflunomide treated mice. Surprisingly, we noted that the residual T cells were enriched for cells with a memory precursor phenotype while effector T cells were strongly reduced. Thus, we hypothesized that leflunomide blocks the expansion and differentiation of effector cells without impacting the formation of memory precursor T cells. Based on this hypothesis, three aims were set for this study:

- In the first part of this study we wanted to confirm the impact of leflunomide on the T cell response during an acute infection. We aimed at validating if leflunomide treatment blocks the differentiation of effector T cells without impairing the formation and functionality of memory precursor and memory T cells.
- The second aim was to address how leflunomide impacts the effector and memory T cell differentiation. We were especially interested to unravel the underlying molecular mechanism and to identify novel regulators, which determine the differentiation of effector and memory T cells during an acute infection.
- Furthermore, we were interested in identifying the time point at which leflunomide causes its impact to ascertain when effector T cells are sensitive to the leflunomide treatment. We also questioned in which phase of the T cell response effector T cells are lost. Thereby we were aiming to determine the branching point at which effector and memory committed T cells segregate.

5. Materials and Methods

Mice

C57BL/6 and Nur77 mice were obtained from Charles River. CD45.1 congenic C57BL/6, OT-1 TCR transgenic mice recognizing Ovalbumin were all obtained from Jackson Laboratory [103]. P14 TCR transgenic mice recognizing the gp33-41 from LCMV were provided by A. Oxenius (ETHZ, Switzerland) [104]. Mice were bred and maintained in SPF facilities and infected mice in conventional or SPF animal facilities.

Experiments were performed in at least 6 week old mice in compliance with the University of Lausanne Institutional and Technical University of Munich regulations and were approved by the veterinarian authorities of the Swiss Canton Vaud and the " Regierung von Oberbayern" in Germany.

Administration of leflunomide and teriflunomide in mice

Starting at day -3 C57BL/6 mice were treated orally with 35mg/kg leflunomide or 20mg/kg teriflunomide every second day. The treatment was stopped at 7 or 28 days post infection. The control mice were treated with Carboxymethylcellulose (CMC).

Leflunomide and teriflunomide suspension

Leflunomide (Arava) and teriflunomide (Aubagio) were purchased from Sanofi.

A tablet of 100mg leflunomide or 14mg teriflunomide was grind up in a mortar and resolved in 0,5 % Carboxymethylcellulose.

Triacetyluridine treatment

Starting at day -3 C57BL/6 mice were treated orally with 35mg/kg leflunomide or Carboxymethylcellulose every second day. Mice receiving the Triacetyluridine treatment were treated with 35mg/kg leflunomide and additionally with 5mg/kg Triacetyluridine (dissolved in PBS). The Triacetyluridine was applied by oral gavage every six hours from day -3 until day 7 post infection.

Infections

Recombinant Listeria monocytogenes stably expressing Ova containing the SIINFEKL (N4) epitope or the APL SIITFEKL (T4) were previously described [105].

Frozen stocks of the Listeria strains were thawed, grown at 37°C in brain-heart infusion broth (Thermo Fisher Scientific) to mid log phase and bacterial numbers were determined by measuring the OD at 600 nm. Naive mice were intravenously injected with 1000–2000 colony forming units (Cfu) Listeria and Listeria immune mice received 100 000 Cfu of Listeria diluted in PBS.

Recombinant Vesicular Stomatitis Virus expressing SIINFEKL were provided by L. Lefrancois [106]. Viruses were grown and titrated on BHK-21 cells. LCMV (strain 53b, Armstrong) was grown and titrated on Vero cells. Frozen stocks were thawed and diluted in PBS. $2x10^6$ plaque forming units (Pfu) VSV or $2x10^5$ Pfu LCMV was injected intravenously (i.v.), or intraperitoneally (i.p.).

Purification of naïve T cells and adoptive T cell transfer

Spleens were mashed through 100µM nylon cell strainers (BD). To eliminate red blood cells, pellets were re-suspended in ACK lysis buffer. For isolation of naive CD8 T cells, the mouse $CD8^+$ T cell isolation kit (Miltenyi Biotech) for untouched $CD8^+$ T cell isolation was used according to the manufacturer's protocol.

Preparation of cell suspensions from spleen and liver

Mice were perfused with PBS. Livers were mashed through a 100µm nylon cell strainer (BD) and re-suspended in 35% physiological percoll solution in DMEM (GE healthcare) and added on top of a 65% percoll solution in PBS. After centrifugation, T cells were harvested from the interphase.

Spleens were mashed through a 100 µm cell strainer and lysed with ACK buffer for 2 min.

CFSE labeling of naïve T cells

$CD8^+$ T cells were purified from spleen as described above. Isolated T cells were labeled using the CellTrace™ CFSE Cell Proliferation Kit from Thermo Fisher Scientific. The cells were incubated in DMEM media with 5µM CFSE for 10min at 37°C. Mice were injected with CFSE labeled cells intravenously.

Isolation of memory T cells

Splenocytes from memory mice were incubated with CD45.1 antibodies conjugated to biotin for 15 min at 4°C. After washing, the pellet was stained for 15 min with anti-biotin beads (Miltenyi Biotech). Cell suspensions were loaded on LS columns and the

flow through was collected. The purity of the isolated cells was determined using the flow cytometry.

Protection assay

For the determination of Listeria load, spleen and liver of Listeria monocytogenes infected mice were collected 4 days after infection in 5ml of lysis buffer (0.1% NP-40 tergitol PBS solution). The organs were mashed in the lysis buffer and serial dilutions were prepared. The dilutions were plated on brain-heart infusion agarose plates containing streptomycin or streptomycin and chloramphenicol. Colonies were enumerated after 24h of growth at 37°C.

Surface and intracellular antibody staining for flow cytometry

For early time points (day1.5- day5) after infection, organs were digested as described above. The organs were mashed through cell strainers and red blood cell lysis was performed using ACK buffer. Blood was collected in heparin containing tubes. Red blood cells were lysed using two rounds of ACK lysis and cell pellets were re-suspended in PBS, 2% FCS, 0.01% Azide (Facs buffer). Unspecific staining was blocked using anti CD16/CD32 antibody (clone 2.4G2). Surface staining was performed for 20-30min at 4°C in Facs buffer containing the following mouse-antibodies (mAb):

CD8 (clone 53-6.7), CD4 (RM4-4 or GK1.5), CD45.1 (A20), CD45.2 (104), CD127 (A7R34 or eBioSB/199), KLRG1 (2F1), CD27 (LG.7F9), CD62L (MEL-14), CD69 (H1.2F3), CD44 (IM7).

Cells were washed twice and fixed for 15 min in PBS, 1% formaldehyde, 2% glucose, 0.03% Azide. For intracellular staining, cells were re-stimulated *in vitro* with Ova peptide (5mM) in the presence of Brefeldin A (7 µg/ml) for the last 4.5 hours. Cells were fixed and permeabilized, using the Cytofix/Cytoperm Kit (BD) and stained with mAbs for IFN-γ (XMG1.2), TNF (MP6-XT22), IL-2 (JES6-5H4) and Granzyme B (without peptide stimulation; GB12). Intracellular transcription factor staining was performed with the Foxp3 / Transcription Factor Staining kit (eBioscience) and stained with anti-TCF-1 (S33966), Eomes (Dan11mag), and T-bet (eBio4B10). For flow cytometry sorting, living cells were stained in Facs buffer.

Antibodies were obtained from from eBioscience, Tonbo, bioXcell, Invitrogen, bioLegend, and BD.

Flow cytometry measurements of cells were acquired on an LSR-Fortessa flow cytometer. Flow cytometry sorting was done with the FACSAriaFusion instrument (BD). All data were analyzed using FlowJo (TreeStar).

In vitro differentiation of IL-2 TE and IL-15 TM cells

T cells were activated with IL-2 (100U/ml) and αCD3/CD28 beads for 3 days. At day 3 post activation IL-2 cells were plated at $1x10^6$ cells/ml in IL-2 media (100U/ml) and IL-15 cells at $2x10^6$ cells/ml in IL-15 (100U/ml). Teriflunomide (100mM; similar concentration as in determined plasma levels of leflunomide treated mice) or DMSO was added and cells were cultured for additional 2 days to generate IL-2 T_E and IL-15 T_M cells.

Glucose tracing

T cells were activated and differentiated *in vitro* in glucose free media (prepped with dialyzed FBS) supplemented with 11 mM glucose. After 4 days, T cells were washed and cultured overnight in media replaced with 11 mM D-[1,2^{13}C] glucose. For harvest, cells were rinsed with cold 0.9% NaCl and metabolites extracted using 1 mL of 80% MeOH kept on dry ice. 10 nM norvaline (internal standard) was added. Following mixing and centrifugation, the supernatant was collected and dried via centrifugal evaporation. Dried metabolite extracts were re-suspended in pyridine and derivatized with methoxyamine (sc-263468 Santa Cruz Bio) for 60 minutes at 37 °C and subsequently with N-(tert-butyldimethylsilyl)-N-methyl-trifluoroacetamid, with 1% tert-butyldimethylchlorosilane (375934 Sigma-Aldrich) for 30 minutes at 80 °C. Isotopomer distributions were measured using a DB5-MS GC column in a 7890 GC system (Agilent Technologies) combined with a 5977 MS system (Agilent Technologies).

Relative quantification of metabolites by LC-MS

T cells were pelleted by centrifugation at -9 °C and washed in 1ml ice cold 3% v/v glycerol solution. Supernatant was removed and cell pellets were flash frozen in liquid N2. For extraction of metabolites 100 µL of extraction solution (80:20 methanol:milli-Q H2O pre-cooled at -80 °C) was added to the pellet, suspended by pipetting up and down and incubated on ice for about 5 min. Extraction mix was

centrifuged at 20.000 *g* for 3 min at -9 °C and supernatant was transferred to fresh eppendorf tubes. 50 µL of extraction solution was added to the pellet, suspend by pipetting up, incubated on ice for about 5 min and centrifuged at 20.000 *g* for 3 min at -9 °C. Supernatant was removed and added to first supernatant. Collected supernatants were centrifuged and 6µl of the supernatants was transferred to a 96 well plate. An equal volume of 13C yeast extract was added to each sample and analyzed by LC-MS. Metabolites were quantified by LC-MS using HILIC Chromatography on a Luna NH2 column on a 1290 Infinity II UHPLC system (Agilent Technologies) combined with targeted detection in a 6495 MS system (Agilent Technologies). Peak areas were normalized to ^{13}C labeled internal standard (ISOtopic Solutions).

Next generation sequencing (NGS)

At day 7 or 28 post infection, splenocytes were enriched for CD45.1$^+$ OT-1 T cells using biotin labeled anti-CD45.1 antibodies and anti-biotin conjugated microbeads in combination with magnetic MACS cell separation (Miltenyi Biotech). High purity (>95%) untouched samples were then obtained by flow cytometry based sorting for CD8$^+$ CD45.1$^+$ OT-1 or CD8$^+$ CD45-1$^+$ CD127$^+$ OT-1 cells. The cells were lysed and RNA was extracted using the Agencourt RNAdvance Cell v2 kit (A47942, Beckman Coulter). RNA integrity number (RIN) and yield were assessed using RNA 6000 Pico Kit (5067-1513, Agilent). Only samples with RIN>8 were used for downstream cDNA synthesis and library preparation. cDNA synthesis and PCR amplification using 1 ng of total RNA from each sample was performed using SMART-Seq v4 Ultra Low Input RNA Kit for Sequencing (634891, Takara/Clontech). After cDNA synthesis, each sample was subjected to 12 cycles of PCR amplification. The generated amplicons were assessed and their concentration was determined with the use of Agilent High Sensitivity DNA Kit (5067-4626, Agilent). 150 pg of the resulting amplified cDNA were used for library preparation with the Illumina Nextera XT DNA Library reagents (FC-131-1024, Illumina). After PCR amplification of the fragmented libraries, the samples were purified with (0.6x) Agencourt AMPure XP beads and eluted in 10 µl of molecular grade water. The quality of the resulting library was assessed with the use of Agilent High Sensitivity DNA Kit (5067-4626, Agilent). The library quantification was performed based on the Illumina recommendations (SY-930-1010, Illumina) with the use of KAPA SYBR FAST qPCR Master Mix (KK4600, Kapa Biosystems). The

samples were sequenced on Illumina HiSeq 2500 system at the following conditions - rapid run, 100 base pairs single-end read, dual-indexed sequencing resulting in 20 million reads per sample.

RNA-seq data processing

Reads were processed using snakemake pipelines [107] as indicated under (https://gitlab.lrz.de/ImmunoPhysio/bulkSeqPipe). Sequencing quality was assessed with fastqc (S, A. FastQC: a quality control tool for high throughput sequence data. http://www.bioinformatics.babraham.ac.uk/projects/fastqc (Version: 0.11.6). Filtering was performed by trimmomatic v0.36 [108] using, mapping by STAR v2.5.3a [109] with genome Mus_musculus.GRCm38, counting by htseq v0.9.1 [110] with annotation Mus_musculus.GRCm38.91. To supervise STAR and fastqc results we used multiqc v1.2 [111].

Bulk RNA-Seq data analysis

Genes with total reads smaller than 10 across all the samples were removed for the differential comparison. Differential expression analysis was performed based on the negative binomial distribution in DESeq2 (version 1.18.1) [112]. Default parameters were used for the analysis. Difference with Basemean greater than 50, absolute log2 fold change larger than 1 and adjust p value smaller than 0.05 were considered significant.

Single-cell RNA-seq

The single-cell RNA-seq was preformed using SCRB-seq protocol, with modifications making it suitable for primary T-cells. The single-cells were sorted on BD FACS Fusion (100 micron nozzle, standard operation settings, single-cell purity, index sorting). Individual cells meeting the gating strategy were sorted directly in lysis buffer into individual wells of a low-binding PCR plate. Immediately after sorting, each plate was spun down, snap-freezed on dry ice and stored at -80oC until use. The single-cell RNA was isolated with the use of magnetic beads and eluted in molecular grade water containing supplemented with RNAse inhibitor. The reverse transcription was performed by adopting the primer strategy described in SCRB-seq, but increasing the length of the

cell barcode to 7 bp. Each single-cell cDNA was amplified in a separate reaction for 22 cycles. The barcoded single-cell amplicons from each plate were pooled and purified with the use of magnetic beads and eluted in molecular grade water. The amplicons quality was assessed with the use of an Agilent High Sensitivity DNA chip. One sequencing library was prepared for each single-cell plate with the use of Illumina Nextera XT DNA library preparation kit. After PCR amplification of the tagmented libraries, they were triple purified (0.6x → 0.6x → 1x) with the use of magnetic beads. The library quality was assessed with the use of an Agilent High Sensitivity DNA chip.

Single-cell RNA-Seq data processing

Cells with less than 500 transcripts or total read count smaller than 5000 were excluded for downstream analysis. A further cell filtering was included to remove cells with highly expressed mitochondrial genes. Read counts were normalized as Counts Per Million (CPM) and top 2000 genes ranked by significance of increase in dropouts were identified based on the depth adjusted negative binomial (DANB) model in M3Drop [113]. Seurat [114] was used for identifying cell subpopulations. Top 10 Principle Components (PCs) and k.para = 200 were used for performing Louvain clustering [115].

Heatmap visualization

Genes for the heatmaps were selected from differentially expressed gene lists of CMC vs Tfl T cells at different time points. Pheatmap (version 1.0.10; Kolde, Raivo, and Maintainer Raivo Kolde. "Package 'pheatmap'." (2015)) was used for the heatmap visualization. Color is encoded by the Z-score based on normalized expression values obtained from DESeq2 (version 1.18.1).

Activation of $CD8^+$ T cells *in vitro*

OT-1 cells were isolated from spleen and seeded into 24-well plates. $1x10^6$ T cells per well were stimulated with anti CD3/CD28 Dynabeads (Invitrogen) and cultured in RPMI supplemented with 10% FCS, penicillin/streptomycin, 5µM 2-ME, and 5mM Hepes (all Invitrogen) in the presence of 50U/ml IL-2 (Chiron). The cells were incubated at 37°C and 5% CO2.

Retrovirus based RNAi

Three shRNA constructs targeting DHODH (TRMSU2000-56749) and one scramble control were obtained in the pLMPd mAmetrine1.1 from transOMIC technologies Inc. (Huntsville, USA).

The sequences for DHODH shRNAs are:

Construct 1:

CTCGAGTGCTGTTGACAGTGAGCGCCCCACTGTCTCTAGATCTAAATAGTGAAG
CCACAGATGTATTTAGATCTAGAGACAGTGGGATGCCTACTGCCTCGGAATTC

Construct 4:

CTCGAGTGCTGTTGACAGTGAGCGCTCCCACTGTCTCTAGATCTAATAGTGAAG
CCACAGATGTATTAGATCTAGAGACAGTGGGATTGCCTACTGCCTCGGAATTC

Construct 6:

CTCGAGTGCTGTTGACAGTGAGCGCGGCCGACTACCTGGTGGTTAATAGTGAA
GCCACAGATGTATTAACCACCAGGTAGTCGGCCATGCCTACTGCCTCGGAATTC

Scrambeld shRNA:

TGCTGTTGACAGTGAGCGAAGGCAGAAGTATGCAAAGCATTAGTGAAGCCACA
GATGTAATGCTTTGCATACTTCTGCCTGTGCCTACTGCCTCGGA

The combination of pLMPd DHODH shRNA-1 and -4 was used for further experiments.

Production of retroviral particles

Recombinant retrovirus was made by transfection of Phoenix-E cells. After reaching approx. 50-60% confluence, Phoenix-E cells were transfected with Fugene.6 according to the manufacturer's protocol. The next day media of Phoenix cells was replaced with new DMEM-10 (DMEM supplemented with 10% FCS, penicillin/streptomycin, 5µM 2-ME, and 5mM Hepes (all Invitrogen)) and further incubated at 32°C. After 48 hours post transfection the virus supernatant was collected.

Transduction of Activated CD8 T Cells

24- 28h post activation the supernatant of activated $CD8^+$ T cells was replaced with 2ml of DMEM-10 media (DMEM supplemented with 10% FCS, penicillin/streptomycin, 5µM 2-ME, and 5mM Hepes (all Invitrogen)) containing the retroviral particles. Polybrene transfection reagent (final concentration 10µg/mL,

Merck Millipore) was added and cells were centrifuged for 90 minutes at 32°C 700xg (2000rpm). After 3-4 hours of incubation, medium was changed and cells were cultured with RPMI-10 and 50 U/ml IL-2 or injected into host mice.

RNA isolation and cDNA synthesis

Transduced $CD8^+$ $Ametrine^+$ T cells were sorted 40-hours post transduction using the FACSAriaFusion instrument (BD). Sorted cells were pelleted by centrifugation at 300 rcf for 5 minutes following re-suspension in 350µL freshly prepared RTL (Lysis Buffer) supplemented with 2-ME. Re-suspended cells were mixed by vortex at maximum speed for 60 seconds and samples were kept at -80°C. For RNA isolation the RNeasy MinElute Cleanup Kit (Qiagen) was used. Samples were thawed at 37°C and 350µL freshly prepared RTL supplemented with 2-ME was added to each sample. After vortexing for 30 seconds, 700µL of 70% freshly prepared MB grade ethanol was added. Samples were shaken vigorously for 15 seconds and the content was transferred to an RNeasy miniElute column and centrifuged for 1 min at 10 000 rcf, RT. The column was washed with 350µL of RWI buffer followed by centrifugation for 30 seconds at 10 000 rcf, RT. 70µL of RDD with 10µL of the reconstituted DNase I were added and 75µL of RDD+DNase solution was transferred onto the column membrane. After 15min incubation, the column was washed with 350µL of RWI. 700µL of RPE was added twice, followed by centrifugation for 1 min at 10 000 rcf, RT and washing of the column with 500µL of 80% freshly prepared MB grade ethanol. The samples were centrifuged with open lid for 5 minutes at 16 000 rcf, RT and the columns were transferred to new low-bind 1,5 mL RNA collection tube. 14µL of MG grade water was added and samples were centrifuged for 1 min at 16 000 rcf, RT.
2µL of extracted RNA samples were aliquoted for running a Bioanalyzer RNA Pico chip. The synthesis of cDNA (ProtoScript® First Strand cDNA Synthesis Kit) was done according to the manufacturers´ protocol.

Real-Time PCR Analysis

TaqMan Real-Time Reverse Transcription-PCR Assay (QIAGEN Real-Time PCR Cycler, Rotor-Gene Q) was performed according to the manufacturer´s protocol (TaqMan® Universal Master Mix II).
The following primers were used:
GAPDH Mm99999915_g1

Rn18s Mm04277571_s1
DHODH Mm00498393_m1
Scrambled vector was used as control.

Cryosections and staining of spleens

Spleens from Listeria monocytogenes or LCMVArm infected mice were harvested at day 7 post infection. The spleens were fixed in paraformaldehyde (4 %) for 4 h and transferred into 30 % sucrose solution overnight. The next day, organs were embedded in OCT-tissue Tek and frozen immediately over liquid nitrogen. The organs were stored at -80 °C. 5 µm sections were cut at -20 and -25 °C using the microtome cryostat (Microm HM 505 E Cryostat, GMI). The sections were air-dried, fixed in -20 °C cold acetone for 5 min and dehydrated with PBS for 5 min at RT. After blocking, CD3 or CD4 (17A2), CD45.R/B220 (RA3-6B2) and CD45.1 (A20) antibodies from Biolegend were used. The staining was performed for 4 h at 4 °C. The slides were mounted with Prolong Gold mounting buffer (Fisher Scientific) and cover slipped. Images were acquired with Leica DMi8 fluorescent microscope (Leica Microsystems) and high-resolution scans were obtained using LAS X Navigator (Leica Microsystems). The images of different channels were merged and exported for analysis (ImageJ). To vectorize the sections a R-script was used. Based on density threshold of the CD3 (T cell zone) and B220 (B cell zone) fluoresces signal, the compartments of the spleen were assessed. The relative distribution of OT-1 T cells in these compartments was determined.

Data analysis

Student's t-test (unpaired, two-tailed) was used to calculate significance levels between groups. p values < 0,05 were considered significant (*p < 0.05; **p < 0.01; ***p <0.001; ****p <0.0001). p values > 0,05 were not significant (ns). Graph generation and statistical analysis was performed using Prism (GraphPad).

6. Results

6.1 Leflunomide impairs T cell expansion without compromising memory formation

The immunosuppressive drug leflunomide is used in the treatment of autoimmune disorders such as rheumatoid arthritis and multiple sclerosis [116]. *In vitro*, leflunomide causes a proliferation arrest of activated lymphocytes by interfering with dihydroorotate dehydrogenase (DHODH) implicated in the de novo pyrimidine synthesis pathway [85]. However, not much is known about how leflunomide impacts T cell responses *in vivo*. Surprisingly, in leflunomide treated patients auto-reactive T cells are efficiently suppressed while patients still retain the ability to react to pathogen-derived antigens [140]. So far, the underlying mechanism of this selective suppression remains largely unknown. Autoimmune disorders are often mediated by low affinity T cells, which bypass central and periphery tolerance mechanism in contrast to high affinity T cells, which dominate immune responses to pathogens [117, 118, 141]. We therefore hypothesized that the sensitivity to leflunomide relies on the different strength of TCR stimulation. Thus, this raised our interest to investigate in more detail how leflunomide impacts the T cell response of low- and high affinity stimulated T cells *in vivo*. To mimic this situation, we adoptively transferred ovalbumin-specific T cells (OT-1), which were stimulated with listeria monocytogenes expressing ligands that gradually differ in the strength of binding to the OT-1 TCR (Figure 7A) into host mice and monitored the $CD8^+$ T cell response. We found that at the peak of the infection leflunomide treatment decreased the percentage of OT-1 T cells by 7 fold regardless whether the cells were stimulated by the high- (N4 (Ova)) or low affinity (T4) ligand (Figure 7B). This clearly excludes an affinity depend action of leflunomide.

The reduction in T cell numbers was consistent in lymphoid and non-lymphoid organs and in different acute infections (Figure 7C, D (only N4 stimulation is shown). Despite the strong suppression of T cell numbers in the effector phase, we surprisingly found, that the percentage but also the total amount of memory OT-1 T cells remained the same in leflunomide treated and untreated mice (Figure 7E, F). These data provided the first evidence that leflunomide blocks the expansion of pathogen-specific T cells while the formation of memory T cells is unaffected.

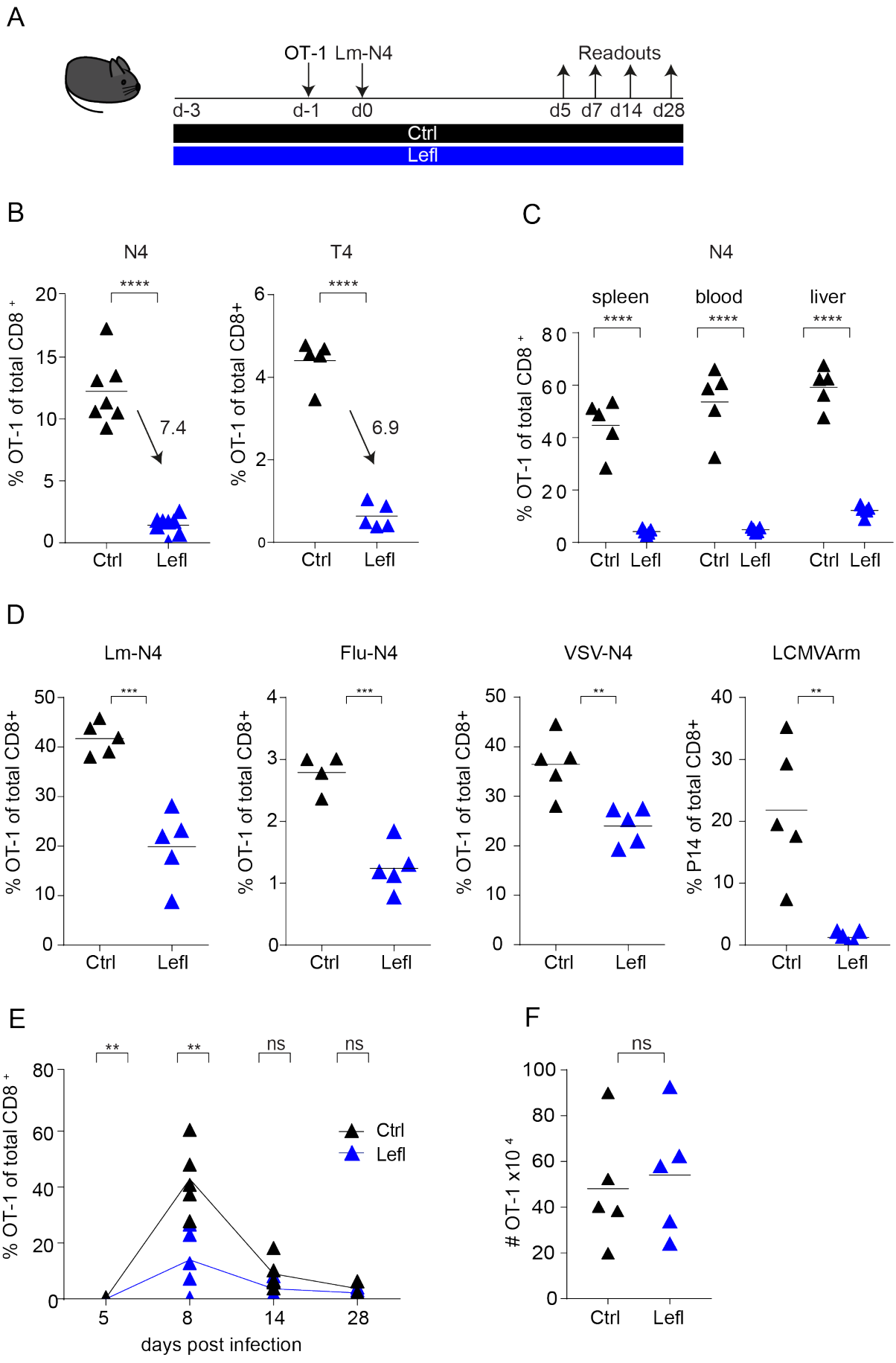
A
OT-1 Lm-N4
Readouts
d-3
d-1
d0
d5 d7 d14 d28
Ctrl
Lefl
B
N4
T4
% OT-1 of total CD8+
7.4
6.9
Ctrl
Lefl
C
N4
spleen
blood
liver
% OT-1 of total CD8+
D
Lm-N4
Flu-N4
VSV-N4
LCMVArm
% OT-1 of total CD8+
% P14 of total CD8+
E
% OT-1 of total CD8+
days post infection
F
OT-1 x10 4
ns

Figure 7. Leflunomide impairs T cell expansion without compromising memory formation

A, Schematic illustration of experimental procedure, C57BL/6 mice were treated with 35mg/kg leflunomide (Lefl) or carboxymethylcellulose (vehicle control, Ctrl) every second day from day -3 until day 7. From day 7 to day 28 post infection, mice were treated every third day with leflunomide or vehicle control. OT-1 T cells were transferred in C57BL/6 hosts at day -1 and infected with listeria monocytogenes (Lm-N4 (high affinity) or Lm-T4 (low affinity)) at day 0. **B**) Mice were analyzed for frequency of OT-1s in the spleen (day 7, Lm-N4 and Lm-T4 infection **C**), for frequency of OT-1s in blood and liver (day 7, Lm-N4 infection **C**) and for frequency of OT-1s in different acute infections (day 7, **D**). **E,** Kinetics of $2x10^4$ transferred OT-1s of Lm-N4 infected C57BL/6 mice treated with Lefl or Ctrl and **F**, total OT-1 numbers in spleen (day 28). Mouse data are representative of at least three independently performed experiments, with at least 5 mice per group. Symbols represent individual mice, with the mean shown. Unpaired t-tests were performed with **p < 0.01; ***p <0.001; ****p <0.0001; ns = not significant (p > 0.05).

6.2 Leflunomide blocks the differentiation of effector T cells while memory precursor are selectively retained

Our first results suggested that leflunomide selectively acts on pathogen- specific effector, but not memory T cells. To further validate our findings, we subsequently analyzed the phenotype of the pathogen-specific T cells by using the marker KLRG1 (Killer cell lectin receptor G1) and CD127 (IL-7 receptor α) that are used in defining effector ($KLRG1^{high}$ $CD127^{low}$) and memory precursor ($KLRG1^{low}$ $CD127^{high}$) $CD8^+$ T cells. Interestingly, at day 7 post infection we made the observation that pathogen-specific OT-1 T cells in leflunomide treated mice contained a higher percentage of memory precursor T cells while the effector T cell population was strongly diminished (Figure 8A). However, the total amount of $KLRG1^{low}$ $CD127^{high}$ memory precursor OT-1 T cells remained constant whereas $KLRG1^{high}$ $CD127^{low}$ effector OT-1 T cells were decreased in leflunomide treated mice in contrast to the corresponding OT-1 T cells in control mice (Figure 8B). Similar observations were made in blood and liver and in an acute LCMVArm, VSV-Ova and Flu-Ova infection (data not shown).
Leflunomide is a pro-drug, which gets converted to its active metabolite teriflunomide. To prove that the observed phenotype is mediated by the active component, we

additionally monitored the T cell response in mice treated with teriflunomide. In line with the leflunomide treatment, teriflunomide blocks the differentiation of effector T cells while the formation of memory precursor T cells is unimpaired (data not shown). The pure active metabolite is much more expensive and has only been used in a few selected experiments.

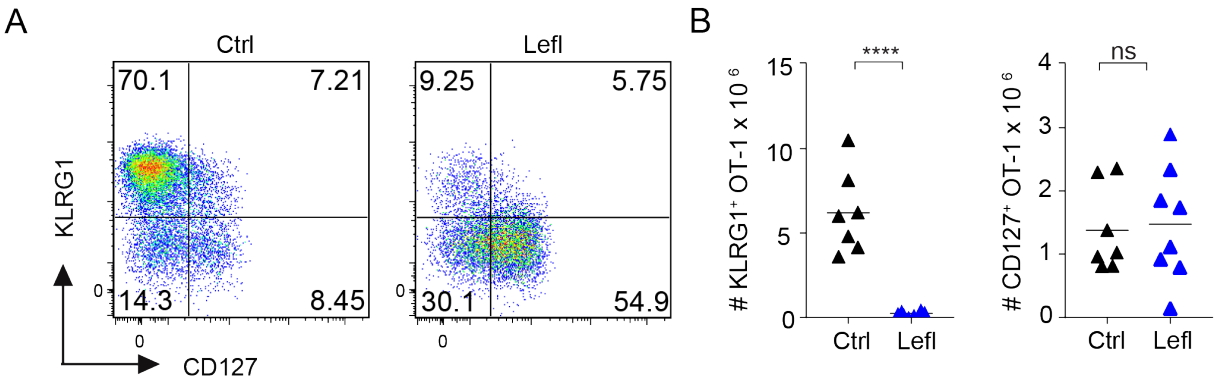

Figure 8. Leflunomide reduces the number of effector but not memory precursor T cells

Phenotypic analysis of OT-1s from Lefl or Ctrl mice in the spleen at day 7 post Lm-N4 infection. **A,** representative dot plots of frequency and **B**, total numbers of KLRG1 and CD127 expressing OT-1s. Mouse data are representative of at least five independently performed experiments with at least 5 mice per group. Symbols represent individual mice, with the mean shown. Unpaired t-tests were performed with ****p <0.0001; ns = not significant (p > 0.05).

We further assessed the phenotype and functionality of antigen-specific $CD8^+$ T cells in treated and untreated mice at day 7 p.i. We found that upon short-term ex-vivo re-stimulation with cognate peptide leflunomide treated and untreated OT-1 T cells responded with comparable IFN-γ and TNF-α secretion patterns (Figure 9A). IL-2, which is robustly secreted by memory $CD8^+$ T cells was higher whereas the effector molecule granzyme B (GrzB) was lower secreted in treated OT-1 T cells (Figure 9A) [119]. Furthermore, treated OT-1 T cells had an increased expression of the lymph node homing receptor L-Selectin (CD62L) (Figure 9B), a higher percentage of Eomes and Tcf1 and a lower percentage of T-bet (Figure 9C) expressing cells.

Effector T cells are preferentially localizing in the red pulp and memory precursor T cells in the T cell zone [17]. In line with this observation, controls OT-1s were mainly located in the red pulp. In contrast, treated OT-1s primarily localized inside the T cell

follicle (Figure 9D) but notably the absolute numbers per area T cell zone remained constant between treated and untreated animals (Figure 9D, bar chart).

Taken all of the results together, these data confirm that memory precursor cells are functional, phenotype and cell number wise retained while T cells with an effector phenotype are diminished in treated mice.

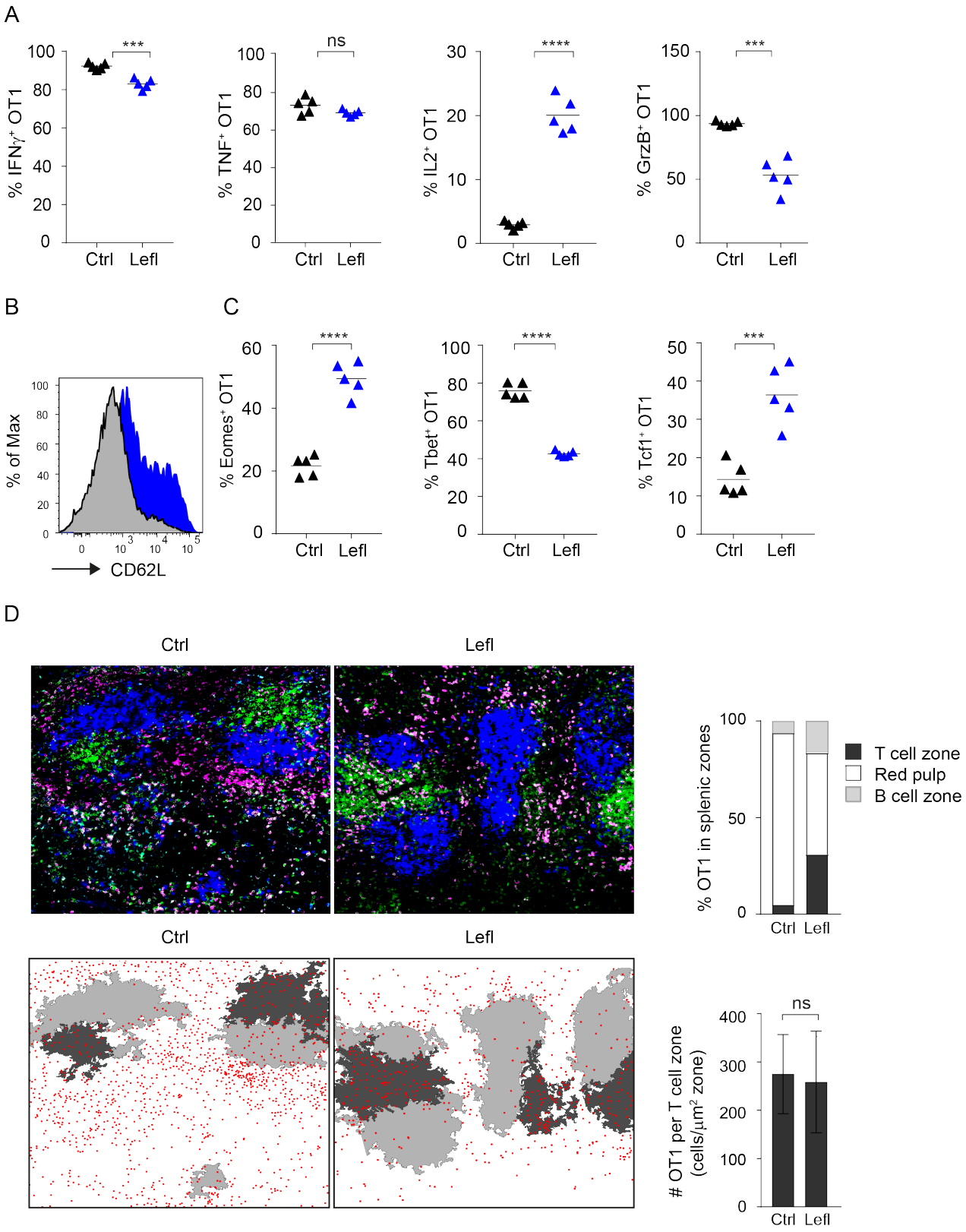

Figure 9. Leflunomide treatment selectively inhibits the differentiation of effector but not memory precursor T cells

Phenotypic characterization of OT-1s from Lefl (blue) or Ctrl (black) mice in the spleen at day 7 post Lm-N4 infection. **A,** Splenocytes were *ex vivo* re-stimulated with Ova-peptide and

stained intracellularly for IFN-γ, TNF-α, IL-2 and GrzB. **B,** Representative histograms of CD62L expressing Lefl (blue) and Ctrl (grey) OT-1 T cells. **C,** Frequency of T-bet, Eomes and Tcf1 expressing OT-1 T cells. **D,** Spleens harvested from Lefl or Ctrl mice engrafted with OT-1s. Sections were stained with anti-B220 (blue), anti-CD3 (green), and anti-CD45.1 (red). Entire spleen sections were recorded using a multicolor-fluorescent slide scanner. The upper row shows representative parts of the scans. The whole section data were then vectorized using a density threshold based algorithm to determine the red-pulp and the T cell and the B cell zone of the white pulp. The lower row shows examples of the vectorized data. Dark grey represents the T cell zone, light grey the B cell zone, and the clear background the red pulp. Red dots mark the location of individual OT-1 T cells. We then determined the fraction of OT-1 T cells in these three anatomical locations. The Graphs show the relative distribution of OT-1s obtained form Lefl or Ctrl treated mice (3 different hosts per group).
Mouse data are representative of at least three independently performed experiments with at least 5 mice per group. Symbols represent individual mice, with the mean shown. Unpaired t-tests were performed with ***p <0.001; ****p <0.0001; ns = not significant (p > 0.05).

6.3 The phenotype and functionality of long- lived memory T cells is unaffected by leflunomide

In previous experiments we could show that the frequency and total numbers of long-lived memory T cells are retained in leflunomide treated mice. We further analyzed the phenotype of memory T cells at day 28 post infection and found that the percentage (Figure 10A) and total numbers (Figure 10B) of KLRG1^{low} CD127^{high} memory T cells differentiated in treated or untreated mice were identical. To further assess the functionality of long-lived memory CD8^{+} T cells we analyzed the *ex-vivo* secretion of IFN-γ, TNF-α and IL-2 after short-term stimulation with cognate peptide. As shown in Figure 10C leflunomide treated and untreated OT-1 T cells responded with comparable IFN-γ, TNF-α and IL-2 secretion patterns.
Thus, in line with the previous obtained result, memory T cells generated in leflunomide treated mice are phenotypically and functionally identical to memory T cells from control mice.

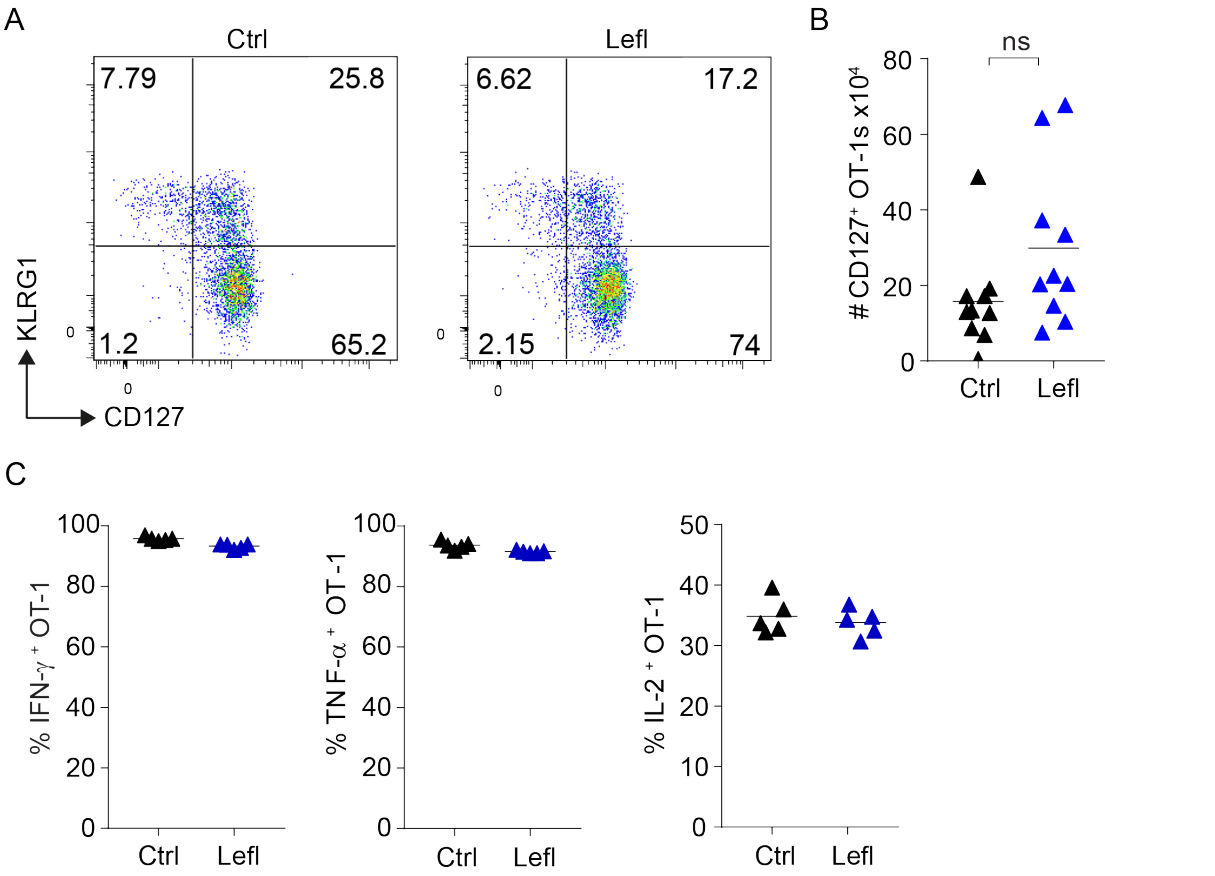

Figure 10. Long-lived memory T cells generated in leflunomide treated and untreated mice are phenotypically and functionally identical

Phenotypic analysis of OT-1s from Lefl or Ctrl mice obtained from the spleen at day 28- day 40 posts Lm-N4 infection. **A,** Representative dot plots of frequency of KLRG1 and CD127 expressing OT-1s. **B**, Total numbers of $CD127^{high}$ $KLRG1^{low}$ memory T cells. **C,** Splenocytes were *ex vivo* re-stimulated with Ova-peptide and stained intracellularly for IFN-γ, TNF-α and IL-2. Mouse data are representative of at least three independently performed experiments with at least 5 mice per group. Symbols represent individual mice, with the mean shown. Unpaired t-test was performed with ns = not significant ($p > 0.05$).

6.4 Memory T cells generated in leflunomide treated mice mediate protective immune responses

Memory $CD8^+$ T cells are an important component of protective immunity [15]. After encountering an antigen in a secondary infection memory T cells rapidly re-expand and mediate protection [120]. Following transfer of isolated memory T cells from treated and untreated mice into new leflunomide untreated hosts, we observed, that

leflunomide or control memory OT-1s had the same re-expansion capability (Figure 11A). Furthermore, analysis of bacterial burden in the spleen and liver of high dose listeria challenged mice indicated that transferred memory T cells from treated and untreated mice showed similar protective capacity compared to mice which didn´t receive memory T cells (Figure 11C). Taken together, these results clearly show that memory function is unaffected by leflunomide.

Leflunomide treatment has an impact on the primary effector T cell response. To examine if a similar effect would be seen in a secondary infection, we adoptively transferred untreated memory T cells in new leflunomide treated or untreated infected hosts. As shown in Figure 11B leflunomide also impacts the expansion of effector T cells in a secondary infection without compromising the formation of secondary memory T cells. Thus, leflunomide regulates both primary and secondary effector T cell responses.

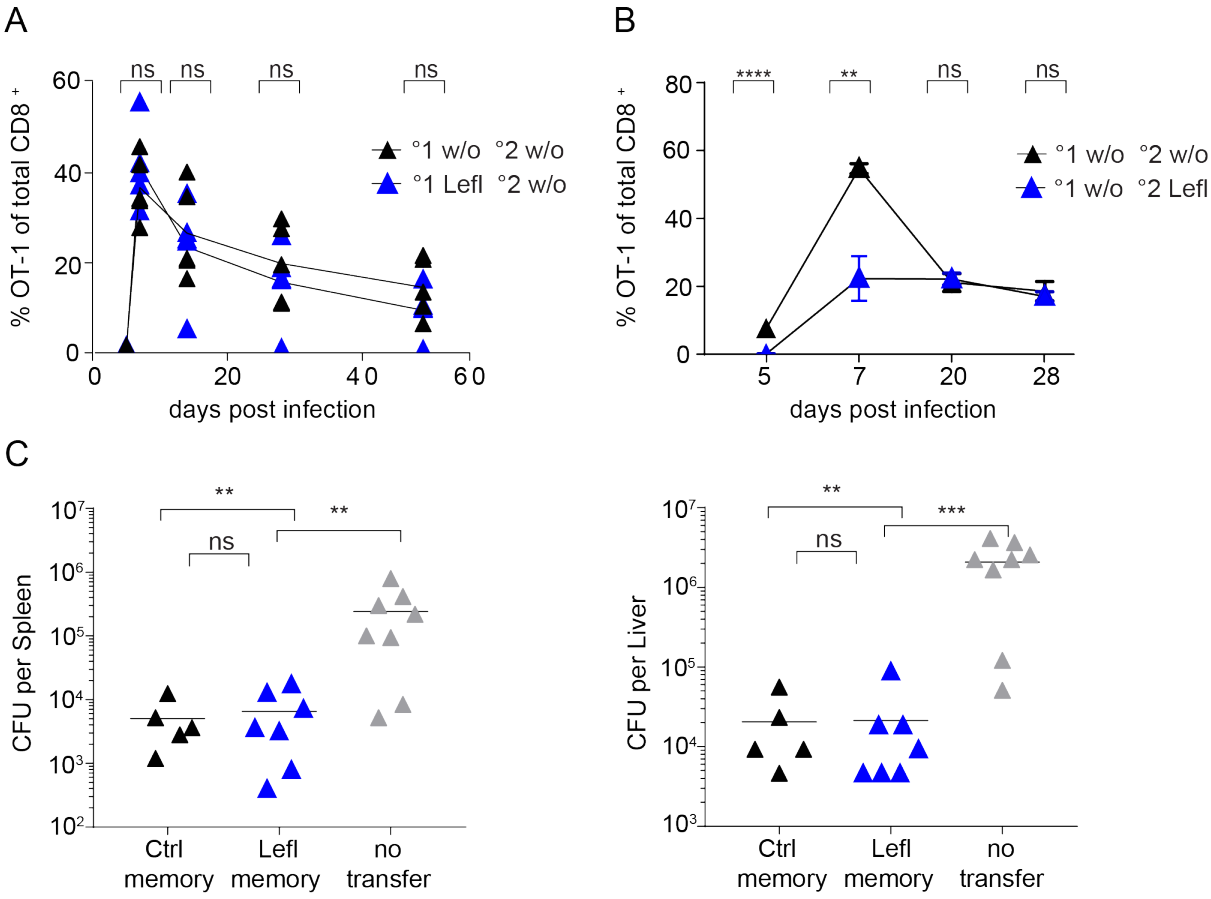

Figure 11. Memory T cells generated in leflunomide treated mice mediate protective immune responses

A, Kinetics of $2x10^4$ memory OT-1s generated in Lefl treated or Ctrl treated mice transferred in new C57BL/6 hosts and infected with 2000 Cfu Lm-N4. **B,** Kinetics of $2x10^4$ memory OT-1s transferred into new C57BL/6 hosts treated with Lefl or Ctrl. **C,** $1x10^5$ splenic memory OT-1s generated in Lefl or Ctrl treated mice were transferred in new C57BL/6 hosts and infected with 10000 Cfu Lm-N4. Colonie forming units per spleen and liver were determined at day 4 post infection (p.i.). Mouse data are representative of at least three independently performed experiments, with at least 5 mice per group. Symbols represent individual mice, with the mean shown. Unpaired t-tests or Mann- Whitney tests were performed with **p < 0.01; ***p <0.001; ****p <0.0001; ns = not significant (p > 0.05).

6.5 Expression of memory signature genes remains unaltered upon teriflunomide treatment

To further assess how the active metabolite impacts effector T cell differentiation, we performed RNA-Seq analysis of sort-purified OT-1 T cells isolated from teriflunomide treated and untreated mice at day 7 and day 28 post infection. Using a fold change difference of 1.5 and false discovery rate (FDR) ≤0.05, we found 629 genes to be up-regulated and 119 genes to be down-regulated in treated OT-1 T cells compared to OT-1 T cells from control mice (Figure 12A). Among the down-regulated genes, *Klrg1* showed a reduced expression in OT-1 T cells from treated mice, as did genes encoding cytotoxic effector molecules, such as *Prf1, Gzma, Gzmk* and *Fasl* (Figure 12A, Heatmap) or the transcriptional regulators Prdm1 and Klf3. In terms of up-regulated genes, treated OT-1 cells showed increased expression of the cell adhesion molecule L-Selectin (*Cd62l*, *Sell*), and other genes associated with memory T cells, including the C-C receptor 7 (*Ccr7*) and the interleukin 2 receptor subunit alpha (*IL-2rα*) as well as the transcriptional regulator *Id3*, *Ezh2*, a histone-lysine N-methyltransferase enzyme and *Myb*. Thus, in line with our previous results these data illustrate that treated and untreated T cells differentially express genes related to terminal effector or memory precursor T cells. To further assess the effect of teriflunomide on the memory precursor and memory T cell subset, we sort-purified KLRG1^{low} CD127^{high} memory precursor OT-1 T cells at day 7 and memory OT-1 T cells at day 28 post infection from treated and untreated mice. Surprisingly but well in line with our previous observations, we did not detect major differences in the gene-profile of KLRG1^{low} CD127^{high} OT-1 T cells at day 7 (Figure 12B) or memory T cells at

day 28 post infection isolated from treated and untreated mice (Figure 12C). These results further highlights that the expression of memory precursor and memory signature genes remains unaltered upon teriflunomide treatment.

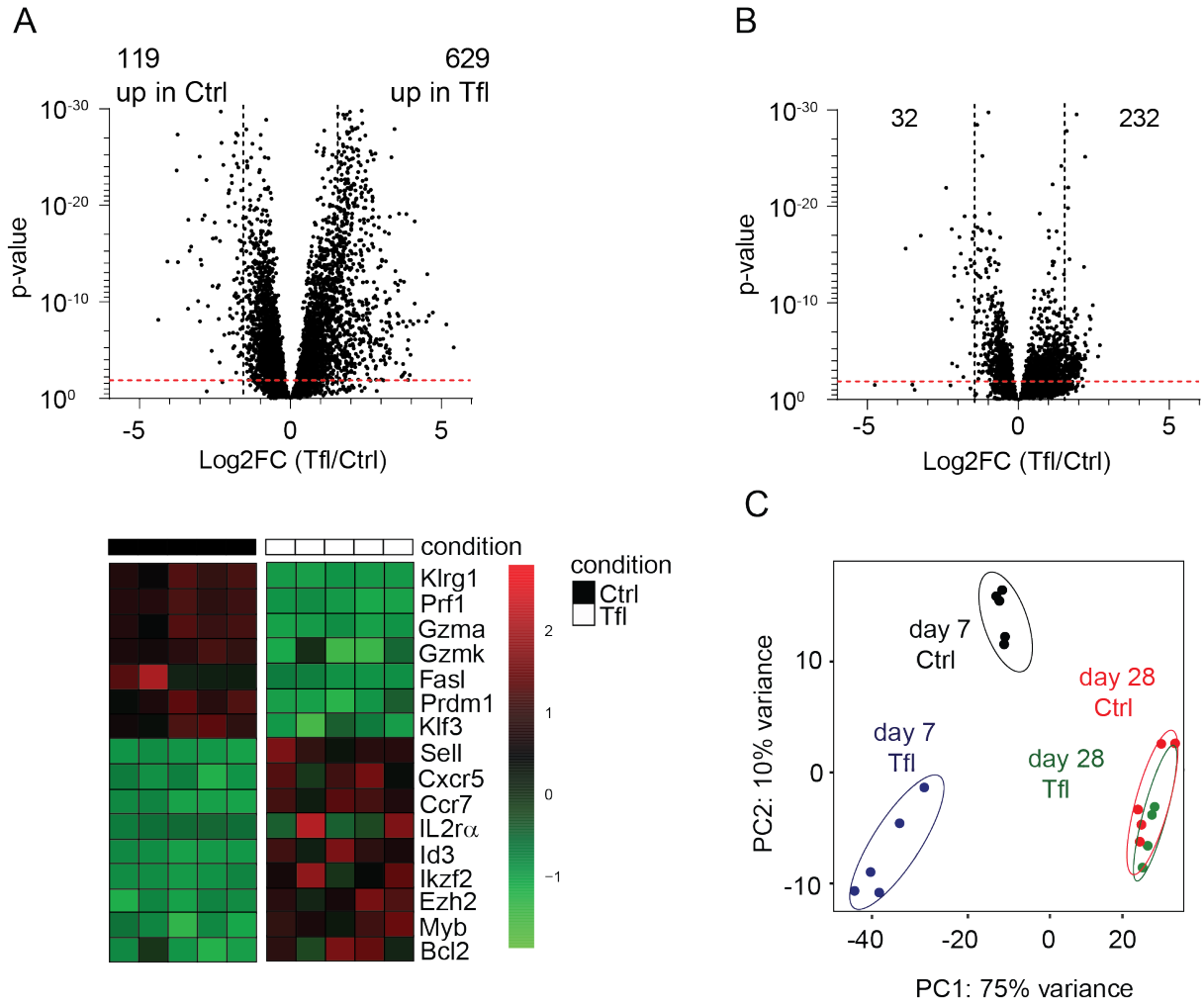

Figure 12. The expression of memory signature genes remains unaltered upon teriflunomide treatment

C57BL/6 mice were treated with teriflunomide (Tfl) or vehicle control (Ctrl), engrafted with $2x10^4$ OT-1 T cells and infected with 2000 Cfu Lm-N4. Splenic OT-1s were re-isolated on day 7 and day 28 p.i. sort purified by flow cytometry and analyzed for gene expression profile using RNA- Seq analysis. **A,** Volcano plot of deregulated genes in treated OT-1s compared to controls at day 7 post infection and heatmap with selected candidate molecules showing differential gene expression. **B,** Volcano plot of deregulated genes in KLRG1^{low} CD127^{high} memory precursor OT-1 T cells from treated mice compared to corresponding T cells from Ctrl mice at day 7 post infection. The volcano plot graphs Log_2 fold-changes against the adjusted p-values. Dashed vertical and horizontal lines reflect the filtering criteria (Log_2

FC = ±1.5 and adjusted value < 0.05). **C,** Comparison of global gene expression of OT-1 T cells isolated from Tfl or Ctrl treated mice at day 7 and day 28 post infection.

6.6 Leflunomide blocks the effector T cell differentiation only during the early T cell activation phase

In all of the experiments leflunomide treatment was applied throughout the acute infection phase. By altering the timing of the leflunomide treatment during activation (blue, day -3) or expansion phase (grey, day 4) (Figure 13A), we aimed to determine the time point at which leflunomide is needed to block the differentiation of effector T cells. As shown in Figure 13, a delayed treatment in the expansion phase (day 4 to day 7 p.i.) leads to a normal effector and memory T cell expansion (B) and differentiation (C, D).

Thus, leflunomide blocks effector T cell differentiation in an early phase of the T cell response, before day 4.

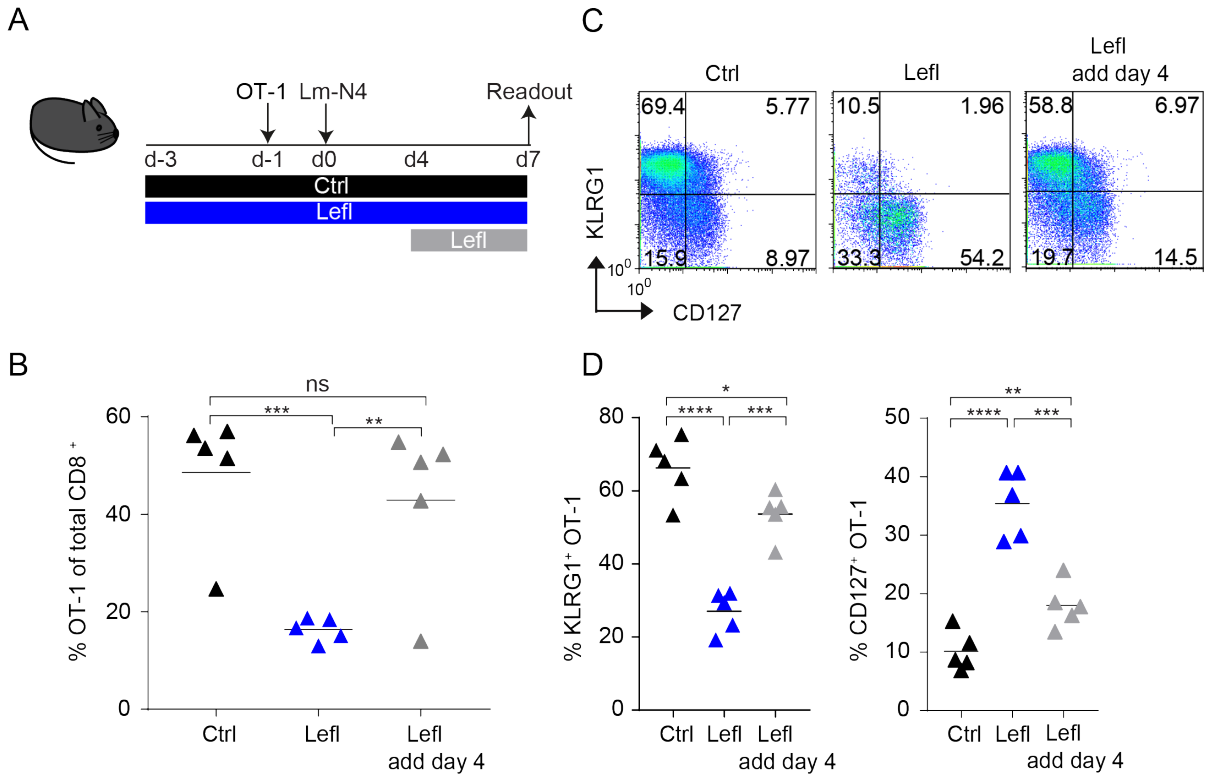

Figure 13. Only early leflunomide treatment blocks the effector T cell differentiation

A, Schematic illustration of experimental procedure. OT-1 T cells were transferred in C57BL/6 hosts at day -1 and infected with 2000 Cfu Listeria monocytogenes (Lm-N4) at day

0. Mice were treated with leflunomide (Lefl, blue) from day -3 to day 7 or from day 4 to day 7 (grey) post infection. As control, mice were treated with vehicle control form day -3 to day 7 (black). Mice were analyzed for frequency (**B**) and KLRG1 and CD127 expression of OT-1s (**C, D**) in the spleen at day 7 post infection.
Mouse data are representative of two independently performed experiments with at least 5 mice per group. Symbols represent individual mice, with the mean shown. Unpaired t-tests were performed with *p <0.05; **p < 0.01; ***p <0.001; ****p <0.0001; ns = not significant (p > 0.05).

To further define the window, in which the T cells are susceptible to the leflunomide treatment, we transferred 30 hours *ex vivo* activated T cells into infected control or leflunomide saturated mice (Figure 14A). Surprisingly, we found that activated T cells were able to robustly expand in leflunomide treated mice (Figure 14B, C). This result further highlights that effector T cells are sensitive to leflunomide only during the early T cell activation phase. Furthermore, since activated T cells are able to still undergo massive proliferation, our observations contrast the view that leflunomide simply inhibits the proliferation of antigen-specific T cells. In contrast, our data indicates the existence of a narrow kinetics window during which the expansion and differentiation of effector T cells can be blocked by leflunomide.

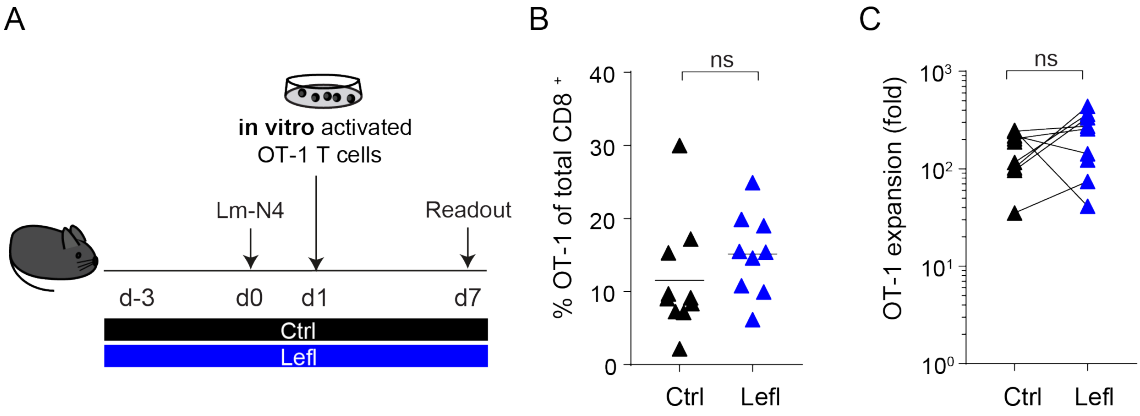

Figure 14. Effector T cells are sensitive to leflunomide only in a narrow kinetics window during the T cell activation phase

A, Schematic illustration of experimental procedure. C57BL/6 mice were treated with leflunomide or vehicle control from day -3 to day 7 and infected with 2000 Cfu Lm-N4 at day 0. OT-1 T cells were activated for 30h *in vitro* and $2x10^5$ OT-1s were transferred into leflunomide treated and infected hosts. **B,** The frequency of OT-1 T cells and **C,** fold

expansion of OT-1s in Ctrl relative to Lefl treated mice was analyzed in spleen (day 7). Engraftment was calculated assuming a 10% “take” of transferred cells.
Mouse data are representative of three independently performed experiments with at least 5 mice per group. Symbols represent individual mice, with the mean shown. Unpaired t-test was performed with ns = not significant ($p > 0.05$).

After a T cell gets stimulated by a suitable antigen, signaling by the T cell receptor (TCR signaling) leads to the activation of T cells. Since leflunomide acts during the early T cell activation we analyzed the expression of the early activation marker CD69 and the immediately up regulated gene Nur77 implicated in early TCR signaling. As shown in Figure 15A, B day 1.5 P14 T cells showed a similar up-regulation of CD69 and Nur77. Along with the down regulated of CD62L (Figure 15C) these data indicate that leflunomide effects the T cell differentiation during T cell priming without acting on early TCR signaling.

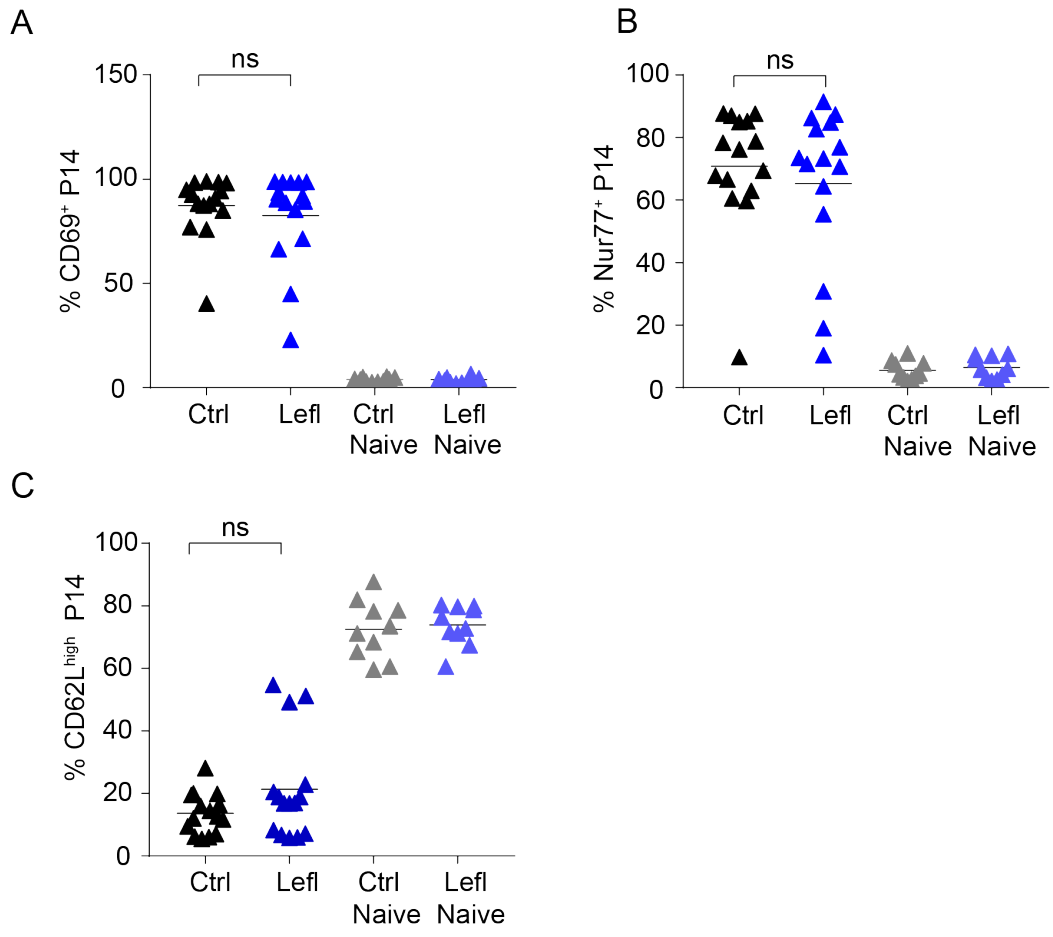

Figure 15. Early TCR signaling is unimpacted in leflunomide treated T cells

A, C57BL/6 mice were treated with leflunomide (Lefl) or vehicle control (Ctrl) as previous described. At day -1 mice were infected with $1x10^5$ LCMVArm and $1x10^6$ Nur77 transgenic P14 T cells were transferred. At day 1.5 post T cell transfer splenic P14s were analyzed for the expression of CD69, Nur77 and CD62L. Data shows the result from three independently performed experiments, with at least 5 mice per group. Symbols represent individual mice, with the mean shown. Unpaired t-test was performed with ns = not significant ($p > 0.05$).

6. 7 Branching into effector and memory precursors occurs early following T cell activation

To ascertain the time point of the T cell response in which leflunomide mediates the block in the effector but not memory T cell differentiation, we analyzed the OT-1 numbers at different time points during the early T cell response (day 1.5- day 5). We noted that the number of antigen-specific T cells is similar during T cell activation (day 1.5) but declines in the early expansion phase (day 3-4) (Figure 16). This suggested that effector T cells are lost following the first divisions and we hypothesized that the branching of effector and memory T cells occurs early after T cell activation.

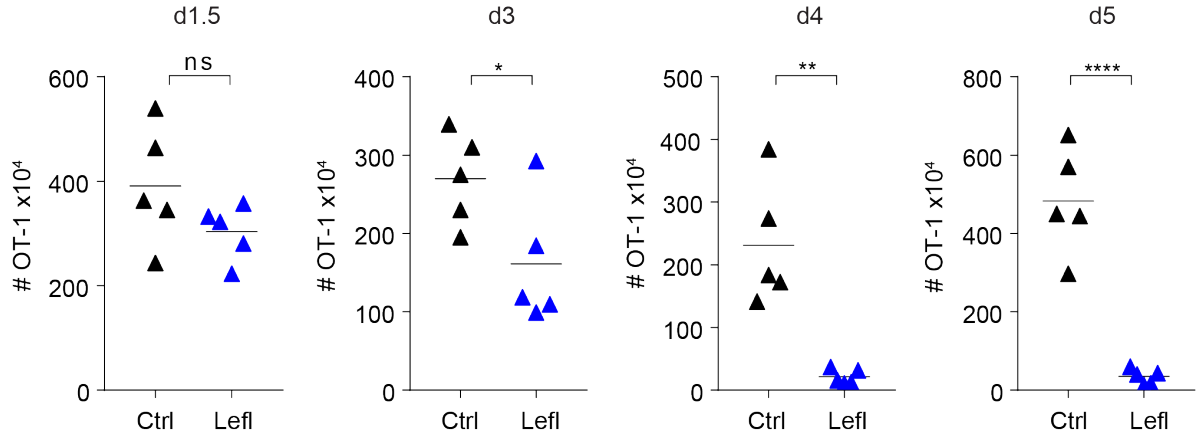

Figure 16. T cell numbers in leflunomide treated mice decline during the first rounds of division following T cell activation

C57BL/6 mice were treated with leflunomide (Lefl) or vehicle control (Ctrl) as previous described. At day 0 OT-1 T cells were transferred (day 1.5: $5x10^5$ day 3, day 4: $1x10^5$ OT-1s, day 5: $2x10^4$ OT-1s) and infected with Lm-N4. At indicated time point's splenic OT-1s were isolated and total numbers determined. Data shows the result from three independently performed experiments, with at least 5 mice per group. Symbols represent individual mice,

with the mean shown. Unpaired t-tests were performed with *p <0.05; **p < 0.01; ****p <0.0001; ns = not significant (p > 0.05).

To prove this hypothesis, we sort-purified single OT-1 T cells at day 4 post infection and performed single-cell RNA sequencing. With the Seurat based clustering approach, we identified four distinct cell populations based on shared or unique patterns of gene expression (Figure 17A). Cluster 1 (green) was equally enriched for OT-1 T cells from control and treated mice (Figure 17B). In line with our observation that treated OT-1 T cells are enriched for memory precursor while control mice mainly contain terminally differentiated effector T cells, we defined T cells in cluster 1 as memory precursor cells. In contrast, cluster 2 (blue) is dominated by T cells from control mice, which we consider to be effector T cells (Figure 17B). Further analysis of differential gene expression shows a massively down regulation of *Pi3k* and *rictor* implemented in the effector- T cell differentiation in cluster 1 (green) (Figure 17C). In contrast, *Foxo1*, which promotes memory T cell differentiation by repression of T-bet mediated effector functions [121] was up regulated in cluster 1 (green), but down regulated in cluster 2-4 (orange, blue, red). *Tbx21* (T-bet) itself is expressed in cluster 2 (blue). Finally, *Socs-3*, which is needed to form memory T cells by inhibition of IL-12 induced STAT4 activation was up- regulated in cluster 1 (green) whereas the expression of *IL-12* was down- regulated [142]. Taken all of the differentially expressed genes into account, it further underlines the enrichment of memory precursor T cells in cluster 1 (green) and effector T cells in cluster 2 (blue). Deregulated genes in cluster 3 (orange) and 4 (red) suggest that these clusters may consist of cells with signatures of effector T cells. Due to up regulation of the cell cycle regulator *Ccnd1* and *Cdc42*, we suggest that cluster 3 (orange) and 4 (red) contains activated precursor T cells dedicated to differentiate into effector T cells (Figure 17C).

Taken all of the results together, we demonstrated that early after activation memory precursor T cells are selectively retained while effector T cells are lost in treated mice. This highlights the early branching of effector and memory T cells during the first rounds of division following T cell activation.

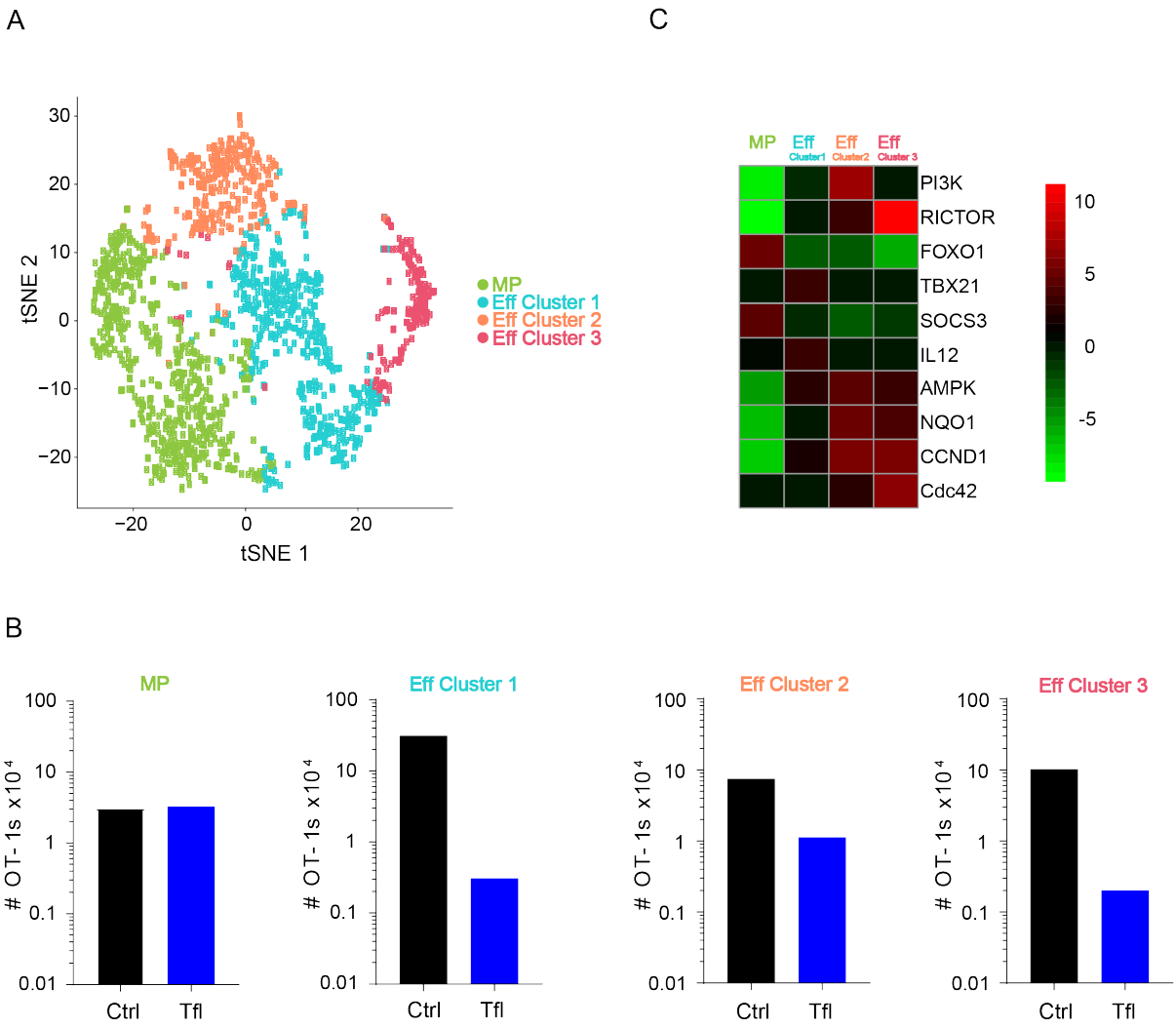

Figure 17. The branching of T cells into effector and memory precursors occurs early following T cell activation

C57BL/6 mice were treated with teriflunomide (Tfl) or vehicle control (Ctrl), engrafted with $1x10^5$ OT-1 T cells and infected with 2000 Cfu Lm-N4. Splenic OT-1s from 5 control and treated animals were re-isolated on day 4 and 1000 single cells were sort purified by flow cytometry. **A**, Seurat t-SNE displayed output for four distinct clusters based on gene expression differences for 1000 T cells demarcated by different colors (Cluster 1: green, cluster 2: blue, cluster 3: orange, cluster 4: red). **B,** Total OT-1 numbers in the different clusters at day 4 p.i. **C,** Ingenuity Pathway Analysis (IPA) approach was used to analyze the differential gene expression between the different clusters. Color is encoded by the IPA activation z- score. Heatmap shows selected candidate molecules. **MP**: Memory precursors, **Eff:** Effector T cells

In search of the explanation why effector but not memory T cells are sensitive to the leflunomide treatment we observed that the metabolic regulator AMP-activated

protein kinase (AMPK) and NQO1, which encodes the NAD(P)H dehydrogenase [quinone] 1 of the respiratory complex were differentially expressed between the memory precursor and effector clusters (Figure 17C). Since the differentiation of effector and memory T cells is linked to different requirements in the metabolism it raised our interest to compare the impact of leflunomide on the metabolism of effector and memory T cells.

6.8 Teriflunomide impacts metabolic profiles of effector but not memory T cells

To investigate the overall effect of the active metabolite of leflunomide on the metabolism of effector and memory $CD8^+$ T cells, we traced ^{13}C labeled glucose, which is differentially metabolized in effector and memory T cells [65]. To obtain a high amount of effector and memory T cells we differentially cultured activated $CD8^+$ T cells in interleukin-2 (IL-2) and interleukin-15 (IL-15) to generate IL-2 effector T cells (T_E) and IL-15 memory T cells (T_M). By tracing the metabolization of ^{13}C- labeled glucose in T_E and T_M cells in the presence or absence of teriflunomide we observed, that the percent of ^{13}C-labeled glycolysis intermediates pyruvate and lactate and the TCA cycle intermediates citrate, malate, fumarate and succinate were significantly reduced in teriflunomide treated T_E cells compared to controls (Figure 18A). The treatment of T_E cells with teriflunomide further lead to a decrease in the frequency of ^{13}C-labeled fatty acids (Palmitate, stearate, fatty acid C18:1) and amino acids and affects the glutaminolysis (Glutamate) (Figure 18A). In contrast, in T_M cells treated with teriflunomide we observed no major differences in the percentage of the ^{13}C-labeled intermediates compared to control treated cells (Figure 18A).
By comparing the cellular levels of metabolites between treated and untreated T cells, we further found that in T_E cells the treatment lead to a strong reduction in glycolysis, TCA cycle, pentose-phosphate pathway, glutaminolysis, fatty acid- and amino acid synthesis intermediates (Figure 18B), whereas the cellular metabolome of T_M cells was not significantly affected (Figure 18B). Furthermore, in treated T_E cells the de novo synthesis of the pyrimidine uracil and the cellular numbers of the nucleoside cytidine and the pyrimidine ribonucleotides CMP, CTP and UTP were reduced compared to controls (Figure 18A, B). Interestingly, the teriflunomide

treatment had only minor effects on the de novo generation or cellular levels of pyrimidine metabolites in T_M cells (Figure 18B).

Taken all of these results together, teriflunomide treatment triggers metabolic changes in effector but not memory T cells, which could result in an effector T cell loss.

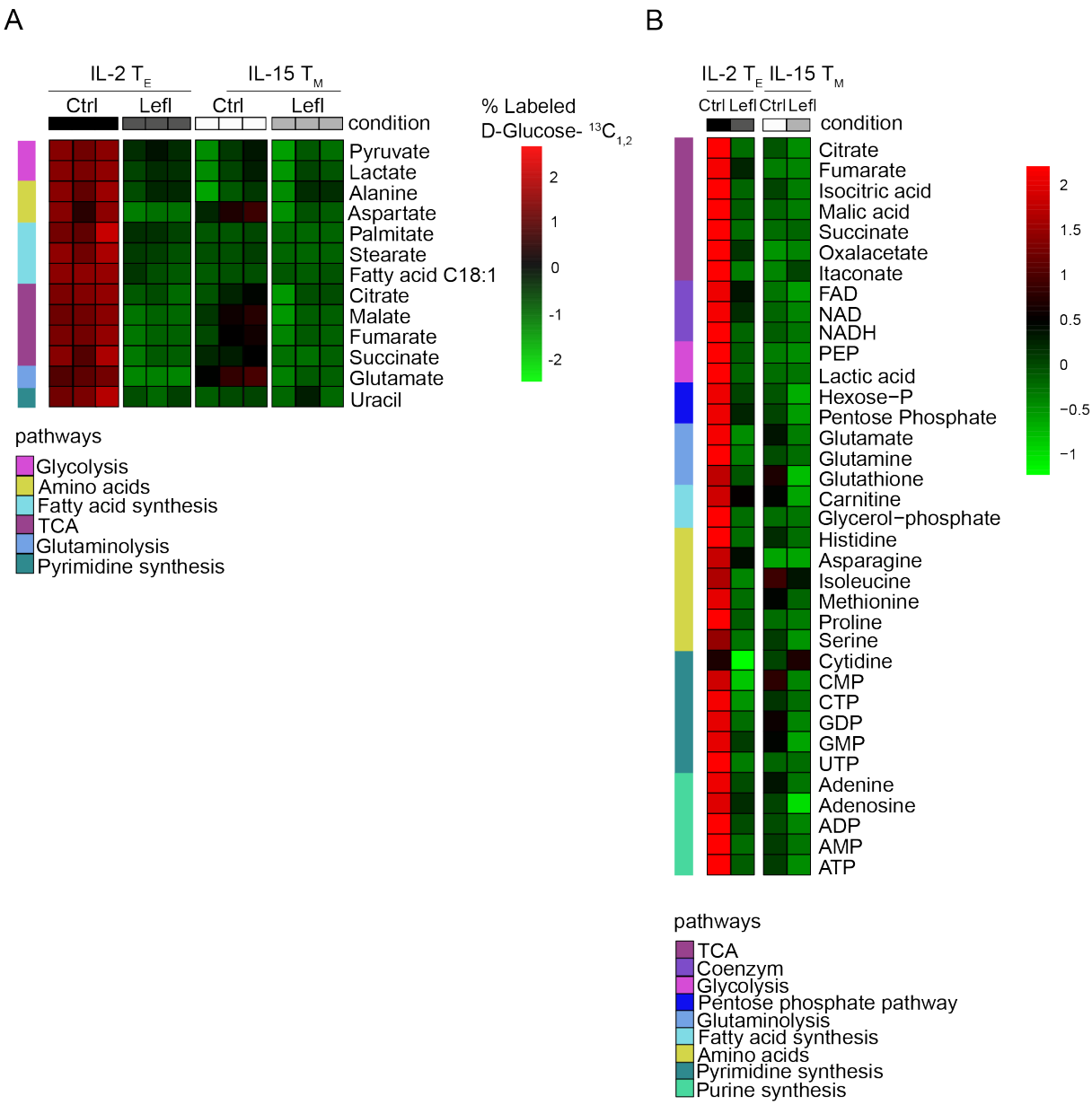

Figure 18. Teriflunomide impacts metabolic profiles of effector but not memory T cells

A, Activated IL-2 T_E and IL-15 T_M cells were treated with teriflunomide (Tfl) or DMSO (Ctrl), cultured overnight with D-Glucose-$^{13}C_{1,2}$ and traced for incorporation by mass spectrometry. Heat map representation of % labeled carbons in listed metabolites. Each lane represents separate samples with a technical replicate. **B,** Activated IL-2 T_E and IL-15 T_M cells were treated with teriflunomide (Tfl) or DMSO (Ctrl) and cellular levels of metabolites were measured by LC-MS. Heat map representation of cellular levels of metabolites. Each lane represents a different condition with combined data from five technical replicates.

6.9 Restricting pyrimidine levels by inhibition of DHODH impairs the differentiation of effector T cells

Leflunomide restricts the level of pyrimidine nucleotides by blocking the activity of dihydroorotate dehydrogenase (DHODH)- an essential enzyme in the de novo pyrimidine synthesis pathway. To prove that the inhibition of DHODH is responsible for the loss of effector T cells in an acute infection, we selectively down- regulated the DHODH expression in $CD8^+$ T cells by shRNA-mediated knockdown. The expression of DHODH was diminished to 10% by two combined DHODH-targeting shRNAs (data not shown). We observed that the inhibition of the DHODH expression leads to a decline in OT-1 numbers (Figure 19A) and KLRG1 expressing T cells (Figure 19B) at day 7 post infection. Along with the relative increase in memory precursor T cells (Figure 19B) this confirms that the down-regulation of the DHODH expression leads to an inhibition in the expansion and differentiation of effector T cells. We further transferred sort-purified memory OT-1 T cells transduced with the shDHODH or shcontrol vector into new infected hosts. In line with the previous result observed in leflunomide treated mice (Figure 11B), we observed a three-fold reduction in OT-1 numbers transduced with the shDHODH construct compared to shcontrol transduced OT-1 T cells (Figure 19C, D). Together, these data proves that the inhibition of DHODH impacts the expansion and differentiation of effector $CD8^+$ T cells.

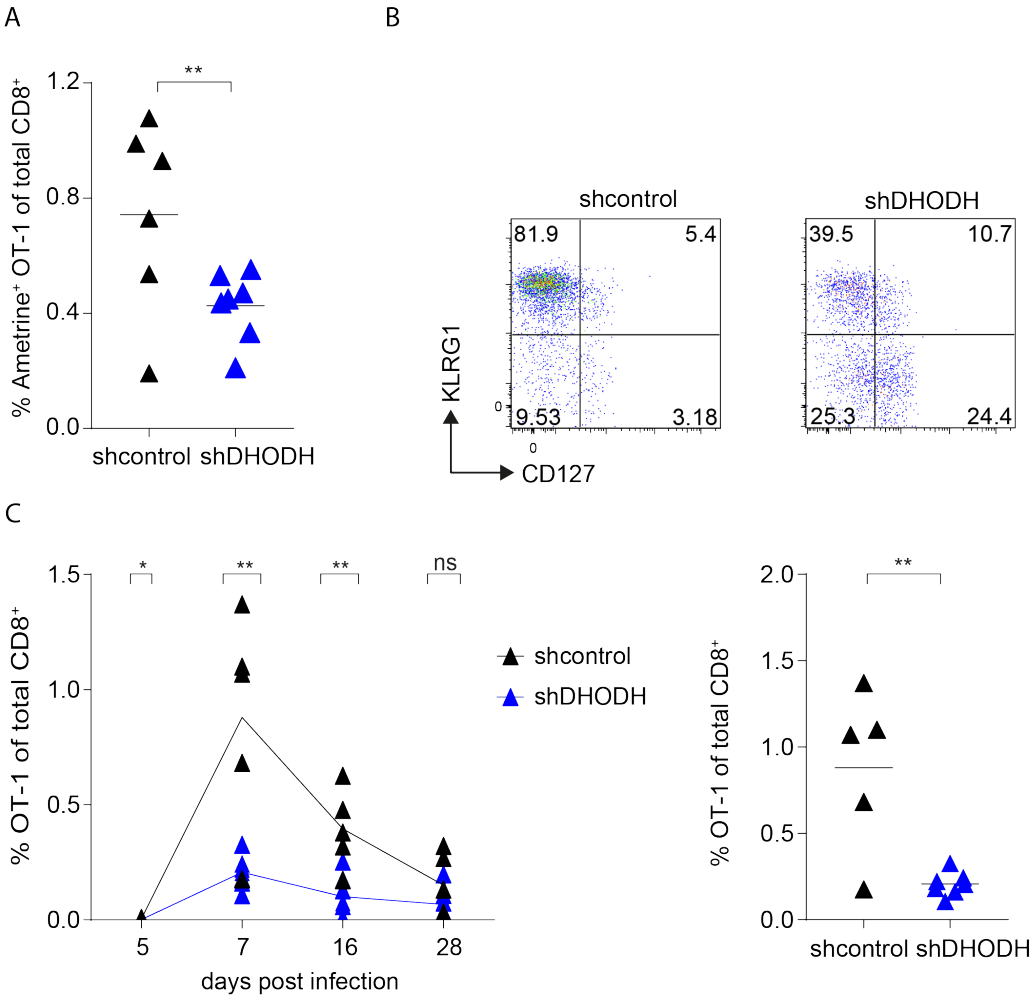

Figure 19. Inhibition of DHODH blocks the differentiation of effector T cells

A, B OT-1 T cells transduced with DHODH knockdown construct (shDHODH) or control vector (shcontrol) were transferred into C57BL/6 mice and infected with 2000 Cfu Lm-N4. The frequency (**A**) and phenotype (**B**) of transduced OT-1 T cells was analyzed at day 7 post infection in the blood. **C,** Kinetics (left) of 5x10^2 Ametrine$^+$ sort purified and transferred memory OT-1s transduced with DHODH knockdown construct or control vector in course of a secondary Lm-N4 infection and frequency at day 7 post infection in the blood (right).

The restriction in pyrimidine levels can be circumvented by the addition of exogenous uridine [80]. Therefore, we treated leflunomide saturated mice with triacetyluridine and analyzed if the differentiation of effector T cells can be rescued. Interestingly, the treatment of mice with triacetyluridine leads to a 4-fold increase in the frequency of OT-1 T cells and a 3-fold increase in KLRG1^{high} CD127^{low} effector T cells compared to mice which only received the leflunomide treatment (Figure 20A, B). Compared to control mice, mice treated with triacetyluridine and leflunomide had a

lower frequency of OT-1 and KLRG1^{high} CD127^{low} effector T cells. The phenotype was consistent in spleen and liver (data not shown). Thus, the exogenous addition of triacetyluridine partially rescues the expansion and differentiation of effector T cells and shows that effector T cells are indeed sensitive to pyrimidine starvation.

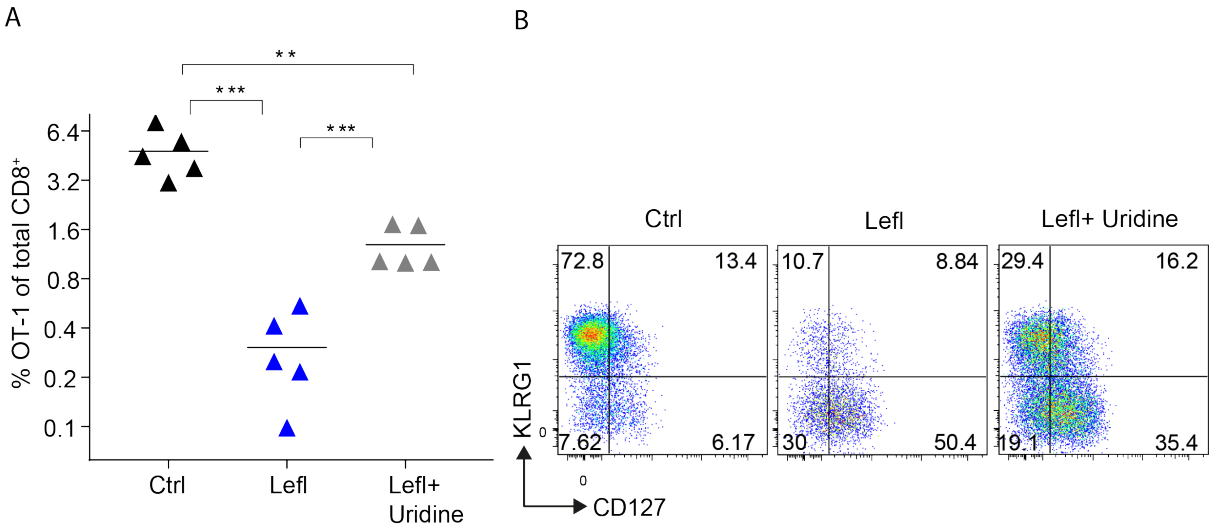

Figure 20. Effector T cells are sensitive to pyrimidine starvation

C57BL/6 mice were treated with control vehicle (black), leflunomide (blue) or 5mg triacetyluridine and leflunomide (grey) from day-3 to day 7 p.i. OT-1 T cells were transferred at day -1 and infected with 2000 Cfu Lm-N4 at day 0. **A,** The frequency of OT-1 T cells and **B,** phenotype was analyzed at day 7 post infection in spleen. Data shows the result from two independently performed experiments, with at least 5 mice per group. Symbols represent individual mice, with the mean shown. Unpaired t-tests were performed with **p < 0.01; ***p <0.001.

The partial rescue of effector T cell differentiation by exogenous addition of pyrimidine derivates raised our interest to further determine the quantitative effect of leflunomide on the de novo synthesis of pyrimidine nucleotides. The observed massive increase in cellular levels of the carbamoyl aspartic acid (CAA) (Figure 21A), a pyrimidine substrate in the de novo pyrimidine synthesis upstream of DHODH in treated T_E and T_M cells demonstrated that leflunomide massively blocks the de novo pyrimidine synthesis.

Since effector T cells are a highly proliferating whereas memory T cells are a quiescent population, we hypothesized that effector T cells are more dependent on the de novo synthesis of pyrimidine nucleotides. The higher amounts of CAA and

uracil in T_E cells indeed highlight, that effector T cells are more dependent on the de novo synthesis of pyrimidines compared to memory T cells (Figure 21B).

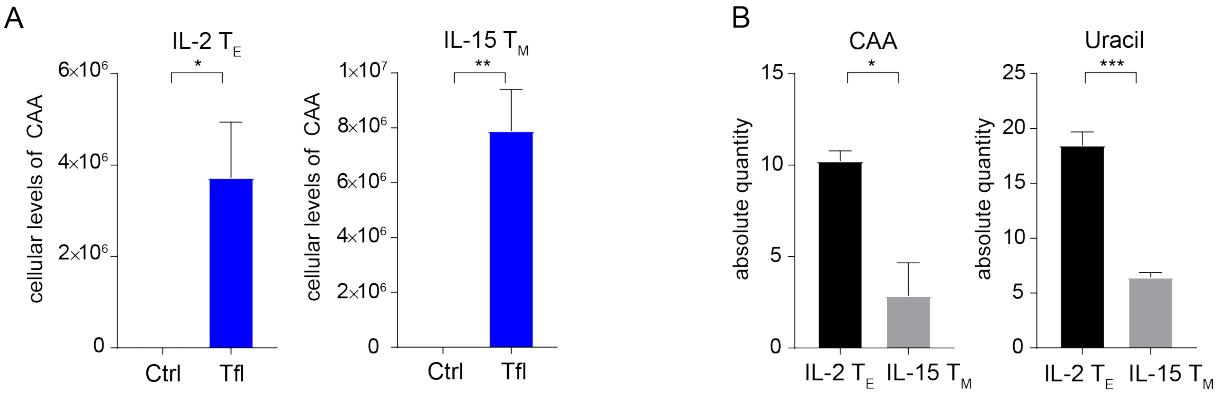

Figure 21. Effector cells are strongly dependent on the de novo pyrimidine synthesis, which is dramatically inhibited by teriflunomide

A, Activated IL-2 T_E and IL-15 T_M cells were treated with teriflunomide (Tfl) or DMSO (Ctrl). Cellular levels of carbamoyl aspartic acid (CAA) in IL-2 T_E (left) and IL-15 T_M (right) were analyzed by LC-MS at day 5 post activation **B,** Activated IL-2 T_E and IL-15 T_M cells were cultured overnight with D-Glucose-$^{13}C_{1,2}$. Absolute quantity of the pyrimidine derivates CAA (left) and uracil (right) at day 5 post activation was determined.

The high dependency on pyrimidine nucleotides by effector T cells can be further explained by the observed proliferation kinetics of activated T cells. In contrast to effector T cells, memory precursor T cells in leflunomide treated mice show a slower rate of proliferation, which could result in a lower demand on nucleotide pyrimidines (Figure 22).

Taken all of the results together, we conclude that the restriction in pyrimidine levels selectively blocks the differentiation of effector but not memory T cells.

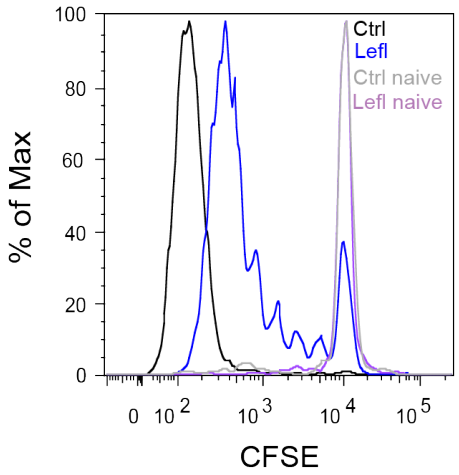

Figure 22. The slower proliferation rate of memory precursors results in a lower demand for de novo synthetized pyrimidines

C57BL/6 mice were treated with leflunomide (Lefl) or vehicle control (Ctrl) as previous described. At day 0 $1x10^6$ CFSE labeled OT-1 T cells were transferred and infected with 2000 Cfu Lm-N4 at day 1. CFSE profile of isolated splenic OT-1s was analyzed at day

3,5 post infection. Naïve OT-1 T cells isolated form infected mice were used as control. Data shows the result from three independently performed experiments, with at least 5 mice per group.

Remark

The experiments shown in Figure 7B and D, Figure 11A and Figure 13 were performed by Susanne Oberle.
The confocal imaging shown in Figure 9D was performed by Madlaina von Hösslin.
Ming Wu analyzed RNA-Seq data and designed heatmaps shown in Figure 12, Figure 17 and 18.
Kristiyan Kanev did the preparation of samples for bulk RNA-Seq and single cell RNA-Seq shown in Figure 12 and 17. He also performed the sort-purification of single cells.
Optimization of the RNA- interferenz method was performed with great help of Zeynep Esencan. She also transduced the T cells with the knockdown or control vectors and FACs analyzed the obtain blood samples shown in Figure 19A and B.
Daniel Puleston performed experiments shown in Figure 18 and 21.

7. Discussion

After the initial antigen-induced activation the progeny of a single naive T cell becomes committed to be either short-lived and die after pathogen clearance or further differentiate into long-lived memory T cells [36, 35]. The mechanisms underlying the differentiation of short-lived effector and long-lived memory T cells have been debated over contrasting models of differentiation [6]. These models involve either a late differentiation, whereby memory $CD8^+$ T cells arise from a subset of effector T cells, or an early branching of the effector and memory T cell lineage [38, 122, 40, 123, 124]. Since suitable markers to identify memory precursors in a population dominated by effector T cells are missing, it is a challenge to verify the differentiation of effector and memory precursor T cells during the T cell expansion phase. In this thesis we demonstrate that the treatment with leflunomide selectively eliminates effector, but not memory precursor, T cells. Along with the finding that treated and untreated memory precursor and memory T cells are transcriptionally, functionally and quantitatively retained, our data strongly suggest that memory precursor T cells do not differentiate in a late linear differentiation from effector T cells. Rather, our comprehensive analysis provides evidence for an early fate specification of effector and memory T cells during the first divisions following T cell activation. In line with our observations, recent single-cell based *in vivo* approaches also assign an early branching of cells into the effector and memory T cell lineage [122, 123]. Whereas Arsenio et al. argues for the model of asymmetric division of T cells, Buchholz et al. suggests an early progressive differentiation of naïve T cells into pre-memory and effector subsets along a non-branching trajectory [122, 123]. Similar to previous work, our data identified the existence of slow proliferating memory precursor and highly proliferating effector T cells during the expansion phase [123]. By simulation Buchholz et al., imply a progressive differentiation of $CD8^+$ T cells, with slowly proliferating memory precursor T cells giving rise to rapidly expanding effector cells [123]. So far, our study does not exclude or favor either the aforementioned models. Further investigations are needed to confirm if our data fits the progressive differentiation model.

In previous studies, similar effector properties of memory precursors and effector T cells as IFN-γ and TNF-α secretion, KLRG1 expression or promoter activation of effector genes, supported the idea of a late differentiation of memory T cells [124]

[40] [37]. In our data day 7 memory precursor T cells retrained in treated mice show similar secretion of Ifn-γ and Tnf-α compared to effector T cells. Thus having similar effector properties might not necessarily counteract against the idea of an early branching of effector and memory T cells. The different conclusions drawn in these studies may be due to a different use of markers or approaches to define effector and memory T cells. While an increased expression of IL-7Rα was the first marker found to distinguish memory precursors from IL7Rα^{low} KLRG1^{high} expressing effector T cells, today the identification of T cells in bulk populations with 'hybrid' phenotypes during the infection further suggests that the diversity of effector and memory CD8$^+$ T subsets is considerably more expansive than previously described [20, 37, 40,119]. However, using the criterion of promoter activation of genes that encode effector proteins to investigate if memory T cells went through an effector phase has the caveat that any activated T cell might be positive simply because it is the descendant of an activated cell, and not a descended from an effector T cell [125]. Furthermore, related-gene expression profiles may also underlie functional similarities as recent principal-component analysis (PCA) of single-cell expression data revealed the closest projection of short-lived effector T cells to effector memory T cells (T_{EM}) [122]. Altogether, further studies are required to demonstrate the stabilities of these T cell subsets based on the aforementioned approaches. Since our study early demarcates memory precursor from dominating effector T cells, it allows for a better dissection of the lineage relationship of effector and memory precursor T cell subsets.

In the last years, the importance of cellular metabolism [68, 126-128] along with the observation that the inhibition of metabolic sensors can impact the CD8$^+$ T cell differentiation opened a new opportunity to specifically target effector- or memory T cells [129, 130]. In this study, we identified that inhibiting DHODH, which results in a pyrimidine starvation, can selectively eliminate effector but not memory T cells. Furthermore, effector T cells are only sensitive to restricted pyrimidine levels in an early narrow window following T cell activation. In line with previous studies, 30 hours *ex-vivo* activated T cells are able to give rise to effector and memory T cells when transferred in leflunomide treated mice [131-133]. Thus, we identified an early metabolic checkpoint that allows for the selective targeting of effector T cells. 12 hours after activation, naïve T cells upregulate essential enzymes in the de novo pyrimidine synthesis, which results in an 8-fold increase in pyrimidine levels over 72

hours of T cell activation [90, 134]. We suggest that these first hours following T cell activation are needed to fuel the observed higher pyrimidine demands in effector T cells as an inadequate nutrient availability is a limiting factor for T cell proliferation, differentiation and function [135]. The partial rescue of effector T cell differentiation in leflunomide and triacetyluridine treated mice further highlights the sensitivity of effector T cells to different pyrimidine levels and suggests the need for a higher concentration of exogenous triacetyluridine to fully compensate the leflunomide mediated block in the pyrimidine synthesis [136]. However, after this early narrow window, T cells may have reached sufficient amount of pyrimidines to expand and differentiate into effector T cells. Leflunomide massively decreased pyrimidine levels not only in effector, but also in memory precursor T cells. In contrast to effector T cells, we show that memory precursor T cells are slow proliferating cells, which could explain their lower demand for pyrimidine nucleotides. In knockdown experiments a ten percent expression of DHODH is needed for the survival of transduced T cells and we concluded, that this expression level could mirror the minimal expression level needed to generate sufficient pyrimdines for the differentiation into memory precursor T cells.

Previous gene profiling analyses indicated that small slow cyclers consist of a memory cell profile and a lower metabolic activity as compared with fast cyclers [137]. Besides modulating pyrimidine levels, we further observed that teriflunomide treatment causes severe metabolic changes in effector but not memory T cells. In the past years several publications reported that following activation, the conversion to an activated effector T cell is marked by a high glycolytic metabolism in contrast to memory T cells, which exhibit a more quiescent metabolic profile [64, 69, 128]. Teriflunomide treatment decreased the use of glucose but also the amount of cellular metabolites in effector T cells needed to fuel their proliferation, cell growth and differentiation. These metabolic changes contrast the previous published demands for differentiation of effector T cells [64, 69]. Recent observations redefine metabolic requirements, as enhancing the glycolytic metabolism through the T cell response impairs the formation of effector cells while long-lived memory $CD8^+$ T cells were formed in similar numbers [138]. In line with our results, the loss of effector T cells due to changes in the metabolism, suggests that effector T cells may have a more defined metabolic requirement. In contrast, memory precursor T cells may better tolerate changes in T cell metabolism and the generation of sufficient ATP and

nutrients, regardless of the source could provide the basal conditions for their differentiation [138]. Studies from Blagih et al. further underline the need of effector T cells to adapt to nutrient starvation via AMP-activated protein kinase (AMPK) to sustain metabolic requirements. Mice lacking AMPK display reduced mitochondrial bioenergetics responses and have a reduced amount of effector T cells [130]. This result could explain why treated day 4 memory precursor T cells with a reduced expression of AMPK and genes involved in cellular respiration are retained in our data whereas effector T cells are lost. Further studies of the impact of alterations in cellular metabolism on fate determination will be necessary to clearly define how early metabolic changes affects T cell differentiation. Moreover, these results suggest the need to clarify, if the changes in the T cell metabolism are indeed caused by the starvation of pyrimidines or through a yet unidentified DHODH mediated mechanism. An experiment, that is being carried out is restricting pyrimdine levels by knockdown of the trifunctional enzyme CAD (carbamoyl-phosphate synthetase 2, aspartate transcarbamylase, and dihydroorotase), located upstream of DHODH in the pyrimidine synthesis pathway. A repetitive block in the effector T cell expansion and differentiation could further confirm the impact of pyrimidine starvation on metabolic changes.

Finally, our results further provide strong implications with clinical relevance. Until today, it is considered that the immunomodulatory action of leflunomide relies on the proliferation inhibition of activated lymphocytes by interfering with the activity of the fourth enzyme in the de novo synthesis of pyrimidine nucleotides, dihydroorotate dehydrogenase (DHODH) [80, 83, 85]. Our study suggests, that leflunomide blocks the expansion and differentiation of cytotoxic effector T cells and thereby dampens autoimmune disorders. Along with our observation, that *ex vivo* pre-activated T cells robustly proliferate in leflunomide saturated mice these results strongly contrast the concept that leflunomide simply interferes with the proliferation of activated T cells. A first analysis of blood samples from multiple sclerosis patients treated with the active metabolite of leflunomide (teriflunomide) confirms our assumption. We found that, the frequency of effector T cells is reduced while memory precursor T cells are retained. Only mild side effects are observed in patients treated with teriflunomide [139]. Nevertheless, due to the formation of memory T cells strong rebounds could be observed after leflunomide treatment interruption. Our studies in mice demonstrate, that memory T cells generate in leflunomide treated mice are able to re-expand and

differentiate into cytotoxic effector T cells when re-stimulated in a leflunomide free environment. Thus, the obtained result further strengthens the uninterrupted use of teriflunomide in patients, or after the treatment was stopped the immediately treatment with other medications to block the re-activation of memory T cells.

Overall perspective

In contrast of the traditional linear differentiation of memory T cells, we argue in favor of the existence of an early differentiation of effector and memory T cells. This early differentiation constitutes a mechanism through which effector, but not memory T cells can be selectively targeted by pyrimidine restriction during the first divisions following T cell activation. Along with the observed changes in the metabolism of effector T cells, we suggest, that the differentiation of effector T cells underlies pre-defined metabolic requirements to sustain proliferation, differentiation and function. We further believe, that comparing the earliest effector and memory precursor T cells can help to clarify the apparent discrepancy of which surface markers, promoter activities or epigenetic markers can be used to identify cells as effector or memory T cells. After all, a better understanding of the effector and memory T cells differentiation is an essential step in the design of vaccinations that could provide protection against various diseases and we strongly envisage that modulating the pyrimidine metabolism of T cells can be a novel and powerful tool to improve T cell based vaccinations.

8. Abbreviation list

A77 1726 teriflunomide
APC antigen presenting cell
APL altered peptide ligand
ATP adenosine triphosphate
CAD trifunctional, multi-domain enzyme (carbamoyl-phosphate synthetase 2, aspartate transcarbamylase, and dihydroorotase)
CD45 common antigen expressed in all leukocytes with two different alleles, CD45.1 and CD45.2.
CFSE carboxyfluorescein succinimidyl ester
Cfu colony forming units
CMC carboxymethylcellulose
CD8 cluster of differentiation 8
DC dendritic cell
DHODH dihydroorotate dehydrogenase
ECAR extracellular acidification rate
ETC electron transport chain
FACS fluorescent activated cell sorting
FAO fatty acid oxidation
FAS fatty acid synthesis
gp33 LCMV derived gp33-41 peptide KAVYNFATC
GrzB granzyme B
HIV human immunodeficiency virus
HCV hepatitis C virus
IFN-γ interferone γ
IL interleukine
i.p. intraperitoneally
i.v. intravenously
KLRG1 killer-cell lectin like receptor G1
LCMV lymphocytic Choriomeningitis Virus
Lefl leflunomide
Lm listeria monocytogenes
Lm-N4 listeria monocytogenes expressing the native ligand Ovalbumin

Lm-T4 listeria monocytogenes expressing the APL T4

LN lymph node

MHC major Histocompatibility Complex

MP memory precursor cells

MS multiple sclerosis

NAD nicotinamid-adenin-dinukleotid

OCR oxygen consumption rate

OT-1 CD8 TCR transgenic cells recognizing SIINFEKL with high affinity

Ova ovalbumin

OXPHOS oxidative phosphorylation

p.i. post infection

P14 CD8 TCR transgenic cells recognizing the LCMV derived KAVYNFATC

Pfu plaque forming units

pMHC major histocompatibility complex bound with a peptide

RA rheumatoid arthritis

SC single cell

SRC spare respiratory capacity

TCA tricarboxylic acid

TCM central memory T cell

TCR T cell receptor

TE effector T cells

TEM effector memory T cell

TM memory T cells

TF transcription factor

Tfl teriflunomide

TNF-α tumor necrosis factor α

TRM tissue resident memory cell

VSV vesicular stomatitis virus

9. Literature

1. Koup, R.A. and D.C. Douek, *Vaccine design for CD8 T lymphocyte responses.* Cold Spring Harbor perspectives in medicine, 2011. **1**(1): p. a007252-a007252.
2. Esser, M.T., et al., *Memory T cells and vaccines.* Vaccine, 2003. **21**(5): p. 419-430.
3. Amanna, I.J. and M.K. Slifka, *Contributions of humoral and cellular immunity to vaccine-induced protection in humans.* Virology, 2011. **411**(2): p. 206-215.
4. Zanetti, M. and G. Franchini, *T cell memory and protective immunity by vaccination: is more better?* Trends in Immunology, 2006. **27**(11): p. 511-517.
5. Obar, J.J. and L. Lefrançois, *Early events governing memory CD8(+) T-cell differentiation.* International Immunology, 2010. **22**(8): p. 619-625.
6. Kaech, S.M. and W. Cui, *Transcriptional control of effector and memory CD8+ T cell differentiation.* Nature Reviews Immunology, 2012. **12**: p. 749.
7. Joshi, N.S. and S.M. Kaech, *Effector CD8 T Cell Development: A Balancing Act between Memory Cell Potential and Terminal Differentiation.* The Journal of Immunology, 2008. **180**(3): p. 1309-1315.
8. Carr, E.L., et al., *Glutamine Uptake and Metabolism Are Coordinately Regulated by ERK/MAPK during T Lymphocyte Activation.* The Journal of Immunology, 2010. **185**(2): p. 1037-1044.
9. Joshi, N.S., et al., *Inflammation Directs Memory Precursor and Short-Lived Effector CD8⁺ T Cell Fates via the Graded Expression of T-bet Transcription Factor.* Immunity, 2007. **27**(2): p. 281-295.
10. Butler, N.S., J.C. Nolz, and J.T. Harty, *Immunologic Considerations for Generating Memory CD8 T Cells through Vaccination.* Cellular microbiology, 2011. **13**(7): p. 925-933.
11. Krummel, M.F., F. Bartumeus, and A. Gérard, *T cell migration, search strategies and mechanisms.* Nature Reviews Immunology, 2016. **16**: p. 193.
12. Curtsinger, J.M. and M.F. Mescher, *Inflammatory cytokines as a third signal for T cell activation.* Current Opinion in Immunology, 2010. **22**(3): p. 333-340.
13. Borthwick, N.J., et al., *Loss of CD28 expression on CD8+ T cells is induced by IL-2 receptor γ chain signalling cytokines and type I IFN, and increases susceptibility to activation-induced apoptosis.* International Immunology, 2000. **12**(7): p. 1005-1013.
14. Mempel, T.R., S.E. Henrickson, and U.H. von Andrian, *T-cell priming by dendritic cells in lymph nodes occurs in three distinct phases.* Nature, 2004. **427**: p. 154.
15. Wherry, E.J. and R. Ahmed, *Memory CD8 T-Cell Differentiation during Viral Infection.* Journal of Virology, 2004. **78**(11): p. 5535-5545.

16. Obst, R., *The Timing of T Cell Priming and Cycling.* Frontiers in Immunology, 2015. **6**: p. 563.
17. Jung, Y.W., et al., *Differential Localization of Effector and Memory CD8 T Cell Subsets in Lymphoid Organs during Acute Viral Infection.* Journal of immunology (Baltimore, Md. : 1950), 2010. **185**(9): p. 5315-5325.
18. Lau, L.L., et al., *Cytotoxic T-cell memory without antigen.* Nature, 1994. **369**: p. 648.
19. Surh, C.D. and J. Sprent, *Homeostasis of Naive and Memory T Cells.* Immunity, 2008. **29**(6): p. 848-862.
20. Kaech, S.M., et al., *Selective expression of the interleukin 7 receptor identifies effector CD8 T cells that give rise to long-lived memory cells.* Nature Immunology, 2003. **4**: p. 1191.
21. Becker, T.C., et al., *Interleukin 15 Is Required for Proliferative Renewal of Virus-specific Memory CD8 T Cells.* The Journal of Experimental Medicine, 2002. **195**(12): p. 1541-1548.
22. Goldrath, A.W., et al., *Cytokine Requirements for Acute and Basal Homeostatic Proliferation of Naive and Memory CD8⁺ T Cells.* The Journal of Experimental Medicine, 2002. **195**(12): p. 1515-1522.
23. Khan, S.H. and V.P. Badovinac, *Listeria monocytogenes: a model pathogen to study antigen-specific memory CD8 T cell responses.* Seminars in immunopathology, 2015. **37**(3): p. 301-310.
24. Zenewicz, L.A. and H. Shen, *Innate and adaptive immune responses to Listeria monocytogenes: A short overview.* Microbes and infection / Institut Pasteur, 2007. **9**(10): p. 1208-1215.
25. Brundage, R.A., et al., *Expression and phosphorylation of the Listeria monocytogenes ActA protein in mammalian cells.* Proceedings of the National Academy of Sciences of the United States of America, 1993. **90**(24): p. 11890-11894.
26. Zhou, X., et al., *Role of Lymphocytic Choriomeningitis Virus (LCMV) in Understanding Viral Immunology: Past, Present and Future.* Viruses, 2012. **4**(11): p. 2650-2669.
27. Kotturi, M.F., et al., *The CD8(+) T-Cell Response to Lymphocytic Choriomeningitis Virus Involves the L Antigen: Uncovering New Tricks for an Old Virus.* Journal of Virology, 2007. **81**(10): p. 4928-4940.
28. Althaus, C.L., V.V. Ganusov, and R.J. De Boer, *Dynamics of CD8⁺ T Cell Responses during Acute and Chronic Lymphocytic Choriomeningitis Virus Infection.* The Journal of Immunology, 2007. **179**(5): p. 2944-2951.
29. Ou, R., et al., *Critical Role for Alpha/Beta and Gamma Interferons in Persistence of Lymphocytic Choriomeningitis Virus by Clonal Exhaustion of Cytotoxic T Cells.* Journal of Virology, 2001. **75**(18): p. 8407-8423.

30. Cobleigh, M.A., et al., *The Immune Response to a Vesicular Stomatitis Virus Vaccine Vector Is Independent of Particulate Antigen Secretion and Protein Turnover Rate.* Journal of Virology, 2012. **86**(8): p. 4253-4261.

31. Lichty, B.D., et al., *Vesicular stomatitis virus: re-inventing the bullet.* Trends in Molecular Medicine, 2004. **10**(5): p. 210-216.

32. Hastie, E., et al., *Oncolytic Vesicular Stomatitis Virus in an Immunocompetent Model of MUC1-Positive or MUC1-Null Pancreatic Ductal Adenocarcinoma.* Journal of Virology, 2013. **87**(18): p. 10283-10294.

33. Badovinac, V.P., J.S. Haring, and J.T. Harty, *Initial TCR-transgenic precursor frequency dictates critical aspects of the CD8 T cell response to infection.* Immunity, 2007. **26**(6): p. 827-841.

34. Moon, J.J., et al., *Tracking epitope-specific T cells.* Nature Protocols, 2009. **4**: p. 565.

35. Stemberger, C., et al., *A Single Naive CD8⁺ T Cell Precursor Can Develop into Diverse Effector and Memory Subsets.* Immunity, 2007. **27**(6): p. 985-997.

36. Gerlach, C., et al., *One naive T cell, multiple fates in CD8(+) T cell differentiation.* The Journal of Experimental Medicine, 2010. **207**(6): p. 1235-1246.

37. Sarkar, S., et al., *Functional and genomic profiling of effector CD8 T cell subsets with distinct memory fates.* The Journal of Experimental Medicine, 2008. **205**(3): p. 625-640.

38. Chang, J.T., et al., *Asymmetric T Lymphocyte Division in the Initiation of Adaptive Immune Responses.* Science, 2007. **315**(5819): p. 1687.

39. Rubinstein, M.P., et al., *IL-7 and IL-15 differentially regulate CD8+ T-cell subsets during contraction of the immune response.* Blood, 2008. **112**(9): p. 3704-3712.

40. Herndler-Brandstetter, D., et al., *KLRG1+ Effector CD8+ T Cells Lose KLRG1, Differentiate into All Memory T Cell Lineages, and Convey Enhanced Protective Immunity.* Immunity, 2018. **48**(4): p. 716-729.e8.

41. Banerjee, A., et al., *The Transcription Factor Eomesodermin Enables CD8(+) T Cells to Compete for the Memory Cell Niche.* Journal of immunology (Baltimore, Md. : 1950), 2010. **185**(9): p. 4988-4992.

42. Takemoto, N., et al., *Cutting Edge: IL-12 Inversely Regulates T-bet and Eomesodermin Expression during Pathogen-Induced CD8⁺ T Cell Differentiation.* The Journal of Immunology, 2006. **177**(11): p. 7515-7519.

43. Danilo, M., et al., *Suppression of Tcf1 by Inflammatory Cytokines Facilitates Effector CD8 T Cell Differentiation.* Cell Reports, 2018. **22**(8): p. 2107-2117.

44. Tiemessen, M.M., et al., *T Cell Factor 1 Represses CD8⁺ Effector T Cell Formation and Function.* The Journal of Immunology, 2014. **193**(11): p. 5480-5487.

45. Jeannet, G., et al., *Essential role of the Wnt pathway effector Tcf-1 for the establishment of functional CD8 T cell memory.* Proceedings of the National Academy of Sciences of the United States of America, 2010. **107**(21): p. 9777-9782.

46. Zhou, X., et al., *Differentiation and persistence of memory CD8(+) T cells depend on T cell factor 1.* Immunity, 2010. **33**(2): p. 229-240.

47. Intlekofer, A.M., et al., *Requirement for T-bet in the aberrant differentiation of unhelped memory CD8(+) T cells.* The Journal of Experimental Medicine, 2007. **204**(9): p. 2015-2021.

48. Martins, G.A., et al., *Blimp-1 directly represses Il2 and the Il2 activator Fos, attenuating T cell proliferation and survival.* The Journal of Experimental Medicine, 2008. **205**(9): p. 1959-1965.

49. Kallies, A., et al., *Blimp-1 Transcription Factor Is Required for the Differentiation of Effector CD8+ T Cells and Memory Responses.* Immunity, 2009. **31**(2): p. 283-295.

50. Rutishauser, R.L., et al., *Blimp-1 promotes terminal differentiation of virus-specific CD8 T cells and represses the acquisition of central memory T cell properties.* Immunity, 2009. **31**(2): p. 296-308.

51. Welsh, R.M., *Blimp-1 as a regulator of CD8 T cell activation, exhaustion, migration, and memory.* Immunity, 2009. **31**(2): p. 178-180.

52. Ji, Y., et al., *Repression of the DNA-binding inhibitor Id3 by Blimp-1 limits the formation of memory CD8+ T cells.* Nature Immunology, 2011. **12**: p. 1230.

53. Masson, F., et al., *Id2-Mediated Inhibition of E2A Represses Memory CD8⁺ T Cell Differentiation.* The Journal of Immunology, 2013. **190**(9): p. 4585-4594.

54. Cannarile, M.A., et al., *Transcriptional regulator Id2 mediates CD8+ T cell immunity.* Nature Immunology, 2006. **7**: p. 1317.

55. Omilusik, K.D., et al., *Sustained Id2 regulation of E proteins is required for terminal differentiation of effector CD8⁺ T cells.* The Journal of Experimental Medicine, 2018.

56. Yang, C.Y., et al., *The transcriptional regulators Id2 and Id3 control the formation of distinct memory CD8+ T cell subsets.* Nature Immunology, 2011. **12**: p. 1221.

57. Wherry, E.J., et al., *Lineage relationship and protective immunity of memory CD8 T cell subsets.* Nature Immunology, 2003. **4**: p. 225.

58. Kaech, S.M. and E.J. Wherry, *Heterogeneity and Cell-Fate Decisions in Effector and Memory CD8⁺ T Cell Differentiation during Viral Infection.* Immunity, 2007. **27**(3): p. 393-405.

59. Intlekofer, A.M., et al., *Effector and memory CD8+ T cell fate coupled by T-bet and eomesodermin.* Nature Immunology, 2005. **6**: p. 1236.

60. Mackay, L.K., et al., *The developmental pathway for CD103+CD8+ tissue-resident memory T cells of skin.* Nature Immunology, 2013. **14**: p. 1294.

61. Masopust, D., et al., *Dynamic T cell migration program provides resident memory within intestinal epithelium.* The Journal of Experimental Medicine, 2010. **207**(3): p. 553-564.

62. Chang, J.T., E.J. Wherry, and A.W. Goldrath, *Molecular regulation of effector and memory T cell differentiation.* Nature immunology, 2014. **15**(12): p. 1104-1115.

63. Patsoukis, N., et al., *The role of metabolic reprogramming in T cell fate and function.* Current trends in immunology, 2016. **17**: p. 1-12.

64. Buck, M.D., D. O'Sullivan, and E.L. Pearce, *T cell metabolism drives immunity.* The Journal of Experimental Medicine, 2015. **212**(9): p. 1345-1360.

65. Palmer, C.S., et al., *Emerging Role and Characterization of Immunometabolism: Relevance to HIV Pathogenesis, Serious Non-AIDS Events, and a Cure.* The Journal of Immunology, 2016. **196**(11): p. 4437-4444.

66. Palmer, C.S., et al., *Glucose Metabolism Regulates T Cell Activation, Differentiation, and Functions.* Frontiers in Immunology, 2015. **6**: p. 1.

67. Almeida, L., et al., *Metabolic pathways in T cell activation and lineage differentiation.* Seminars in Immunology, 2016. **28**(5): p. 514-524.

68. Chang, C.-H., et al., *Posttranscriptional Control of T Cell Effector Function by Aerobic Glycolysis.* Cell, 2013. **153**(6): p. 1239-1251.

69. Pearce, E.L., et al., *Fueling Immunity: Insights into Metabolism and Lymphocyte Function.* Science, 2013. **342**(6155).

70. Kruger, N.J. and A. von Schaewen, *The oxidative pentose phosphate pathway: structure and organisation.* Current Opinion in Plant Biology, 2003. **6**(3): p. 236-246.

71. Patra, K.C. and N. Hay, *The pentose phosphate pathway and cancer.* Trends in biochemical sciences, 2014. **39**(8): p. 347-354.

72. Hanson, K., et al., *The anti-rheumatic drug, leflunomide, synergizes with MEK inhibition to suppress melanoma growth.* Oncotarget, 2018. **9**(3): p. 3815-3829.

73. Li, E.K., L.-S. Tam, and B. Tomlinson, *Leflunomide in the treatment of rheumatoid arthritis.* Clinical Therapeutics, 2004. **26**(4): p. 447-459.

74. Maddison, P., et al., *Leflunomide in rheumatoid arthritis: recommendations through a process of consensus.* Rheumatology, 2005. **44**(3): p. 280-286.

75. Aly, L., B. Hemmer, and T. Korn, *From Leflunomide to Teriflunomide: Drug Development and Immuno-suppressive Oral Drugs in the Treatment of Multiple Sclerosis.* Current Neuropharmacology, 2017. **15**(6): p. 874-891.

76. Osiri, M., et al., *Leflunomide for the treatment of rheumatoid arthritis.* Cochrane Database of Systematic Reviews, 2002(3).

77. Zhang, C. and M. Chu, *Leflunomide: A promising drug with good antitumor potential.* Biochemical and Biophysical Research Communications, 2018. **496**(2): p. 726-730.

78. Chu, M. and C. Zhang, *Inhibition of angiogenesis by leflunomide via targeting the soluble ephrin-A1/EphA2 system in bladder cancer.* Scientific Reports, 2018. **8**(1): p. 1539.

79. Allison, A.C., *Immunosuppressive drugs: the first 50 years and a glance forward.* Immunopharmacology, 2000. **47**(2): p. 63-83.

80. Cherwinski, H.M., et al., *The immunosuppressant leflunomide inhibits lymphocyte proliferation by inhibiting pyrimidine biosynthesis.* Journal of Pharmacology and Experimental Therapeutics, 1995. **275**(2): p. 1043-1049.

81. Mladenovic, V., et al., *Safety and effectiveness of leflunomide in the treatment of patients with active rheumatoid arthritis.* Arthritis & Rheumatism, 1995. **38**(11): p. 1595-1603.

82. Rozman, B., *Clinical Pharmacokinetics of Leflunomide.* Clinical Pharmacokinetics, 2002. **41**(6): p. 421-430.

83. Fox, R.I., et al., *Mechanism of Action for Leflunomide in Rheumatoid Arthritis.* Clinical Immunology, 1999. **93**(3): p. 198-208.

84. Kalden, J.R., et al., *The efficacy and safety of leflunomide in patients with active rheumatoid arthritis: A five-year followup study.* Arthritis & Rheumatism, 2003. **48**(6): p. 1513-1520.

85. Breedveld, F. and J. Dayer, *Leflunomide: mode of action in the treatment of rheumatoid arthritis.* Annals of the Rheumatic Diseases, 2000. **59**(11): p. 841-849.

86. Quéméneur, L., et al., *Differential Control of Cell Cycle, Proliferation, and Survival of Primary T Lymphocytes by Purine and Pyrimidine Nucleotides.* The Journal of Immunology, 2003. **170**(10): p. 4986-4995.

87. Okesli, A., C. Khosla, and M.C. Bassik, *Human pyrimidine nucleotide biosynthesis as a target for antiviral chemotherapy.* Current Opinion in Biotechnology, 2017. **48**: p. 127-134.

88. Fang, J., et al., *Dihydro-orotate dehydrogenase is physically associated with the respiratory complex and its loss leads to mitochondrial dysfunction.* Bioscience Reports, 2013. **33**(2): p. e00021.

89. Liu, S., et al., *Structures of human dihydroorotate dehydrogenase in complex with antiproliferative agents.* Structure, 2000. **8**(1): p. 25-33.

90. Rückemann, K., et al., *Leflunomide Inhibits Pyrimidine de Novo Synthesis in Mitogen-stimulated T-lymphocytes from Healthy Humans.* Journal of Biological Chemistry, 1998. **273**(34): p. 21682-21691.

91. Dimitrova, P., J.R. Kalden, and H. Schulze-Koops, *Leflunomide: an immunosuppressive drug with multiple effects on T cell function.* Modern Rheumatology, 2002. **12**(3): p. 195-200.

92. Dimitrova, P., et al., *Restriction of De Novo Pyrimidine Biosynthesis Inhibits Th1 Cell Activation and Promotes Th2 Cell Differentiation.* The Journal of Immunology, 2002. **169**(6): p. 3392-3399.

93. Ringshausen, I., et al., *The immunomodulatory drug Leflunomide inhibits cell cycle progression of B-CLL cells.* Leukemia, 2007. **22**: p. 635.

94. Sykes, D.B., et al., *Inhibition of Dihydroorotate Dehydrogenase Overcomes Differentiation Blockade in Acute Myeloid Leukemia.* Cell, 2016. **167**(1): p. 171-186.e15.

95. Liu, L., et al., *Inactivation/deficiency of DHODH induces cell cycle arrest and programed cell death in melanoma.* Oncotarget, 2017. **8**(68): p. 112354-112370.

96. Siemasko, K., et al., *Inhibition of JAK3 and STAT6 Tyrosine Phosphorylation by the Immunosuppressive Drug Leflunomide Leads to a Block in IgG1 Production.* The Journal of Immunology, 1998. **160**(4): p. 1581-1588.

97. Thomas, M., et al., *Inhibition of the epidermal growth factor receptor tyrosine kinase activity by leflunomide.* FEBS Letters, 1993. **334**(2): p. 161-164.

98. Xu, X., et al., *Inhibition of Protein Tyrosine Phosphorylation in T Cells by a Novel Immunosuppressive Agent, Leflunomide.* Journal of Biological Chemistry, 1995. **270**(21): p. 12398-12403.

99. Liu, Z.-G., et al., *Apoptotic signals delivered through the T-cell receptor of a T-cell hybrid require the immediate–early gene nur77.* Nature, 1994. **367**: p. 281.

100. Fujii, H., et al., *Functional dissection of the cytoplasmic subregions of the IL-2 receptor betac chain in primary lymphocyte populations.* The EMBO Journal, 1998. **17**(22): p. 6551-6557.

101. Elder, R.T., et al., *The immunosuppressive metabolite of leflunomide, A77 1726, affects murine T cells through two biochemical mechanisms.* The Journal of Immunology, 1997. **159**(1): p. 22-27.

102. Manna, S.K. and B.B. Aggarwal, *Immunosuppressive Leflunomide Metabolite (A77 1726) Blocks TNF-Dependent Nuclear Factor-κB Activation and Gene Expression.* The Journal of Immunology, 1999. **162**(4): p. 2095-2102.

103. Hogquist, K.A., et al., *T cell receptor antagonist peptides induce positive selection.* Cell, 1994. **76**(1): p. 17-27.

104. Pircher, H., et al., *Viral escape by selection of cytotoxic T cell-resistant virus variants in vivo.* Nature, 1990. **346**: p. 629.

105. Zehn, D., S.Y. Lee, and M.J. Bevan, *Complete but curtailed T-cell response to very low-affinity antigen.* Nature, 2009. **458**: p. 211.

106. Kim, S.-K., et al., *Generation of mucosal cytotoxic T cells against soluble protein by tissue-specific environmental and costimulatory signals.* Proceedings of the National Academy of Sciences, 1998. **95**(18): p. 10814-10819.

107. Köster, J. and S. Rahmann, *Snakemake—a scalable bioinformatics workflow engine.* Bioinformatics, 2018. **34**(20): p. 3600-3600.

108. Bolger, A.M., M. Lohse, and B. Usadel, *Trimmomatic: a flexible trimmer for Illumina sequence data.* Bioinformatics (Oxford, England), 2014. **30**(15): p. 2114-2120.

109. Dobin, A., et al., *STAR: ultrafast universal RNA-seq aligner.* Bioinformatics (Oxford, England), 2013. **29**(1): p. 15-21.

110. Anders, S., P.T. Pyl, and W. Huber, *HTSeq--a Python framework to work with high-throughput sequencing data.* Bioinformatics (Oxford, England), 2015. **31**(2): p. 166-169.

111. Ewels, P., et al., *MultiQC: summarize analysis results for multiple tools and samples in a single report.* Bioinformatics (Oxford, England), 2016. **32**(19): p. 3047-3048.

112. Love, M.I., W. Huber, and S. Anders, *Moderated estimation of fold change and dispersion for RNA-seq data with DESeq2.* Genome biology, 2014. **15**(12): p. 550-550.

113. Andrews, T.S. and M. Hemberg, *Modelling dropouts for feature selection in scRNASeq experiments.* bioRxiv, 2017.

114. Satija, R., et al., *Spatial reconstruction of single-cell gene expression data.* Nature Biotechnology, 2015. **33**: p. 495.

115. Meo, P.D., et al. *Generalized Louvain method for community detection in large networks*. in *2011 11th International Conference on Intelligent Systems Design and Applications*. 2011.

116. Herrmann, M.L., R. Schleyerbach, and B.J. Kirschbaum, *Leflunomide: an immunomodulatory drug for the treatment of rheumatoid arthritis and other autoimmune diseases.* Immunopharmacology, 2000. **47**(2): p. 273-289.

117. Zehn, D. and M.J. Bevan, *T Cells with Low Avidity for a Tissue-Restricted Antigen Routinely Evade Central and Peripheral Tolerance and Cause Autoimmunity.* Immunity, 2006. **25**(2): p. 261-270.

118. Enouz, S., et al., *Autoreactive T cells bypass negative selection and respond to self-antigen stimulation during infection.* The Journal of Experimental Medicine, 2012. **209**(10): p. 1769-1779.

119. Cui, W. and S.M. Kaech, *Generation of effector CD8(+) T cells and their conversion to memory T cells.* Immunological reviews, 2010. **236**: p. 151-166.

120. Kaech, S.M. and R. Ahmed, *Memory CD8(+) T cell differentiation: initial antigen encounter triggers a developmental program in naïve cells.* Nature immunology, 2001. **2**(5): p. 415-422.

121. Rao, Rajesh R., et al., *Transcription Factor Foxo1 Represses T-bet-Mediated Effector Functions and Promotes Memory CD8⁺ T Cell Differentiation.* Immunity, 2012. **36**(3): p. 374-387.

122. Arsenio, J., et al., *Early specification of CD8+ T lymphocyte fates during adaptive immunity revealed by single-cell gene-expression analyses.* Nature Immunology, 2014. **15**: p. 365.

123. Buchholz, V.R., et al., *Disparate Individual Fates Compose Robust CD8⁺ T Cell Immunity.* Science, 2013. **340**(6132): p. 630-635.

124. Youngblood, B., et al., *Effector CD8 T cells dedifferentiate into long-lived memory cells.* Nature, 2017. **552**: p. 404.

125. Ahmed, R., et al., *The precursors of memory: models and controversies.* Nature Reviews Immunology, 2009. **9**: p. 662.

126. Buck, Michael D., et al., *Mitochondrial Dynamics Controls T Cell Fate through Metabolic Programming.* Cell, 2016. **166**(1): p. 63-76.

127. Pearce, E.L., et al., *Enhancing CD8 T-cell memory by modulating fatty acid metabolism.* Nature, 2009. **460**: p. 103.

128. van der Windt, G.J.W. and E.L. Pearce, *Metabolic switching and fuel choice during T-cell differentiation and memory development.* Immunological reviews, 2012. **249**(1): p. 27-42.

129. Araki, K., et al., *mTOR regulates memory CD8 T-cell differentiation.* Nature, 2009. **460**: p. 108.

130. Blagih, J., et al., *The Energy Sensor AMPK Regulates T Cell Metabolic Adaptation and Effector Responses In Vivo.* Immunity, 2015. **42**(1): p. 41-54.

131. Kaech, S.M. and R. Ahmed, *Memory CD8+ T cell differentiation: initial antigen encounter triggers a developmental program in naïve cells.* Nature Immunology, 2001. **2**: p. 415.

132. van Stipdonk, M.J.B., E.E. Lemmens, and S.P. Schoenberger, *Naïve CTLs require a single brief period of antigenic stimulation for clonal expansion and differentiation.* Nature Immunology, 2001. **2**: p. 423.

133. Mercado, R., et al., *Early Programming of T Cell Populations Responding to Bacterial Infection.* The Journal of Immunology, 2000. **165**(12): p. 6833-6839.

134. Fairbanks, L.D., et al., *Importance of Ribonucleotide Availability to Proliferating T-lymphocytes from Healthy Humans: DISPROPORTIONATE EXPANSION OF PYRIMIDINE POOLS AND CONTRASTING EFFECTS OF DE NOVO SYNTHESIS INHIBITORS.* Journal of Biological Chemistry, 1995. **270**(50): p. 29682-29689.

135. Amersfoort, J. and J. Kuiper, *T cell metabolism in metabolic disease-associated autoimmunity.* Immunobiology, 2017. **222**(10): p. 925-936.

136. Weinberg, M.E., et al., *Enhanced Uridine Bioavailability Following Administration of a Triacetyluridine-Rich Nutritional Supplement.* PLoS ONE, 2011. **6**(2): p. e14709.

137. Kinjyo, I., et al., *Real-time tracking of cell cycle progression during CD8+ effector and memory T-cell differentiation.* Nature Communications, 2015. **6**: p. 6301.

138. Phan, A.T., et al., *Constitutive Glycolytic Metabolism Supports CD8(+) T cell Effector Memory Differentiation During Viral Infection.* Immunity, 2016. **45**(5): p. 1024-1037.

139. Oh, J. and P.W. O'Connor, *Teriflunomide in the treatment of multiple sclerosis: current evidence and future prospects.* Therapeutic Advances in Neurological Disorders, 2014. **7**(5): p. 239-252.

140. Yoo, H.-G., et al., *Risk factors of severe infections in patients with rheumatoid arthritis treated with leflunomide.* Modern Rheumatology, 2013. **23**(4): p. 709-715.

141. Zehn, D., S.Y. Lee, and M.J. Bevan, *Complete but curtailed T-cell response to very low-affinity antigen.* Nature, 2009. **458**: p. 211.

142. Cui, W., et al., *An Interleukin-21- Interleukin-10-STAT3 Pathway Is Critical for Functional Maturation of Memory CD8⁺ T Cells.* Immunity, 2011. **35**(5): p. 792-805.

10. Appendix

10.1 Acknowledgement

I would like to thank my supervisor Prof. Dr. Dietmar Zehn for giving me the opportunity to do my PhD thesis in his group. I am very grateful for the stimulating scientific atmosphere and the experimental freedom I had. I thank him for the great time, his permanent openness for discussions and his unlimited support in scientific but also private matters.

I am greatly thankful to Dr. Robert Nechanitzky, who introduced me to Prof. Dr. Dietmar Zehn and supported me through my diploma and PhD thesis.

I would like to thank everybody who provided reagents, technical advice, help and support throughout the years, especially Dr. Susanne Oberle, Dr. Daniel Utzschneider, Francesca Alfei, Kristiyan Kanev, Madlaina von Hösslin, Jolie Cullen and Ming Wu.

I thank my family for their unlimited support. Finally, I would like to thank my husband Dr. Issam Outaleb for his great support and patience during my PhD.

أنت أفضل ما يمكن أن يحدث لي